GEOLOGY AND GEOCHEMISTRY OF ROCKS AND BANDED IRON FORMATION OF NORTHERN PART OF WONAKA SCHIST BELT, NORTHWESTERN NIGERIA

BY

ABDULLAHI USMAN MUHAMMAD

DEPARTMENT OF GEOLOGY

FACULTY OF SCIENCE

AHMADU BELLO UNIVERSITY, ZARIA NIGERIA

DECEMBER, 2014

GEOLOGY AND GEOCHEMISTRY OF ROCKS AND BANDED IRON FORMATION OF NORTHERN PART OF WONAKA SCHIST BELT, NORTH WESTERN NIGERIA

BY

ABDULLAHI USMAN MUHAMMAD B.Sc. (ABU) 2002

M.SC/SCI/10137/2008/2009

A THESIS SUBMITTED TO THE SCHOOL POSTGRADUATE STUDIES, AHMADU BELLO UNIVERSITY ZARIA, IN PARTIAL FULFILMENT OF THE REQUIREMENTS FOR THE AWARD OF DEGREE OF MASTER OF SCIENCE

(M.Sc.) GEOLOGY (MINERAL EXPLORATION)

DEPARTMENT OF GEOLOGY

AHMADU BELLO UNIVERSITY

ZARIA

DECEMBER, 2014.

DECLARATION

I declare that the work in this thesis entitled **Geology and Geochemistry of Rocks and Banded Iron Formation of Northern Part of Wonaka Schist Belt, NW Nigeria** has been carried out by me in the Department of Geology.

The information derived from the literature has been duly acknowledged in the text and a list of references provided. No part of this thesis was previously presented for another degree or diploma at this or any other University.

ABDULLAHI USMAN MUHAMMAD …….....

Name of Student Signature Date

CERTIFICATION

This Thesis entitled ‘’GEOLOGY AND GEOCHEMISRTY OF ROCKS AND BANDED IRON FORMATION OF NORTHERN PART OF WONAKA SCHIST BELT NW NIGERIA’’ by Abdullahi Usman Muhammad meets the regulations governing the award the degree of Master of Science of Ahmadu Bello University, Zaria and is approved for its contribution to knowledge and literary presentation.

…… …….

Chairman, Supervisory Committee Date

……. ……

Member, Supervisory Committee Date

…… ……

Head of Department Date

……. …….

Dean Postgraduate School Date

DEDICATION

I dedicate this work to my late beloved Mother, Rabi'at Usman Muhammad for her encouragement. May her gentle soul rest in perfect peace, Ameen.

ACKNOWLEDGEMENTS

I want to use this opportunity to thank The Almighty ALLAH, THE BENEFICIENT, and THE MERCIFUL for making this work reality.

My sincere gratitude goes to my Supervisors Dr A.A. Ibrahim and Prof. U.A. Danbatta for their tireless supervision, useful suggestions, patience encouragement and constructive criticisms throughout the period of this work

I sincerely wish to acknowledge all the lecturers in the Geology Department for their assistance in one way or the other towards the successful completion of this project. They include Prof. I Garba, Prof. I.I. Funtua, Prof. K.Schoneich, Prof. P.M. Zaborski, Dr. H. Hamza, Dr. P.O. Ogunleye, Dr. .E.A. Bala, Dr. M.L. Garba, Dr. S.A. Alagbe, Dr. E.A. Ikpokonte, Dr. I. Hamidu, Dr. V.E. Obiosio, Dr. T. Najime, Mr. S. Magaji, Dr. I. Yusuf, Dr A. Yola, Dr. J. Ayok, Mr. I. Ahmed and Mr. S.Elatipo. The Technical staff of the Department are not left out and these include Mr. A. Amuda , Mr. J. Ekah, Mr. R. Lamja.

My appreciation also goes to my course mates and other students of the Department. These include Abdullahi Kana, Mr . A. AbdulMuheed, Mr. J.A. Usman.

I am also greatly indebted to my beloved wife Malama Nafisa and our two lovely kids Usman Abdullahi (Papa) and Rabi'at Usman for their patience and understanding during my absence from home as a result of this work. I must also appreciate my Father Alh. Usman Muhammad and my brothers Mal. Lawal Usman, Aliyu Usman, my Sisters Malama Maryam Usman, Amina Usman, Fatima Usman and Fatima Usman (Junior) for their advice, understanding, financial support and always being there for me.

I wish to also appreciate all my good friends that supported me in one way or the other. They include Dr. M.B. Tijjani of Microbiology Department, Ahmadu Bello University, Zaria. Auwal Abubakar Tureta of the Ministry of Solid Minerals and Environment, Zamfara State who provided me with a befitting accommodation during my field work; Mal Suleman, a field assistant, Abubakar Muhammad Yabo, Abdullahi Musa (Bobo), my colleagues in the Office; B.Y. Mohammed, K. Abdulsalam, B. Bako, Ibrahim Malam , A. Alhaji , S.J. Wakawa and above all my former and present Commanding Officers Cdr. A.J. Ahar (ACC) and B.A. Maigari(ACC) respectively for their understanding and support and so many others numerous to mention.

ABSTRACT

Whole rock geochemical analyses using XRF technique as well as flame photometry were carried out major, trace elements and alkali concentrations determination respectively. The data obtained were interpreted using the GCD kit (3.0) software. Petrographic studies of the major rock types reveal the presence of Biotite, Quartz, feldspars as major minerals, while muscovite, garnet, hornblende and tourmaline occur as accessory minerals. In addition, magnetite and manganese are present in the Banded iron formation, the BIF. The area is underlain by rocks of different lithologies ranging from Granite-gneiss, gneiss, schist, Banded Iron Formations, hornfels, greenstone, granodiorites and granites as major rock types while diorite, phyllites and laterites occur as minor lithologies. The granitic gneiss at Kwatarkwashi, biotite muscovite schist and green-stone have sedimentary protholiths, while gneiss, hornfels, granodiorite, medium-grained biotite granite and porphyritic granite are from igneous protholith.

The present work has shown the presence of iron in the belt in the form of BIF with Fe (41.62 wt%), Mn (4.37 wt %) and Al_2O_3 (5.29 wt%) contents comparable to other BIF's in the country such as the BIF's from Malumfashi schist belt (Tudun kudu and Unguwar Malam Ayuba), Birnin-Gwari schist belts and in Isanlu, Central Nigeria. The BIF currently discovered through this work is of submarine to hydrothermal origin and is of silicate facie type.

This study documented the presence placer gold deposits in the belt. Artisanal gold mining activities is currently going-on in the belt at the north-eastern part of the study area at Koha and Butsa villages within River Gajere that flows in SE-NW direction.

TABLE OF CONTENTS

CERTIFICATION iv
DEDICATION v
ACKNOWLEDGEMENTS vi
ABSTRACT viii
LIST OF APPENDICES xvi
CHAPTER 1 1
GENERAL INTRODUCTION 1
1.1 DEFINITIONS 1
1.2 LOCATION AND ACCESSIBILTY 2
1.3 RELIEF AND DRAINAGE 3
1.4 CLIMATE, VEGETATION AND LAND USE 5
1.5 PREVIOUS WORK 5
1.6 AIM AND OBJECTIVES OF PRESENT WORK 6
1.7 RESEARCH METHODOLOGY 7
1.7.1 Field Mapping 7
1.7.2 Sampling and Sample Preparation 7
1.7.3 X-Ray Fluorescence (XRF) 8
1.7.4 Flame Photometry 9
2.2.1 The Migmatites-gneiss-quartzite complex 14
Table 1: A generalized geochronology for the basement rocks of Nigeria (modified after McCurry, 1976; Dada, 1997) 15
2.2.2 Schist Belts 16
2.2.4 Minor Felsic and Mafic Intrusives 19
CHAPTER 3 21
FIELD GEOLOGY AND PETROGRAPHY 21
3.1 INTRODUCTION 21
3.2 GRANITIC- GNEISS 21
3.2.1 Megascopic Description 24
3.2.2 Microscopic Description 24

3.3 GNEISS 26
3.3.1 Megascopic Description 26
3.3.2 Microscopic Description 26
3.4 BIOTITE- MUSCOVITE SCHIST 27
3.4.1 Megascopic Description 30
3.4.2 Microscopic Description 30
3.5 THE BANDED IRON FORMATION (BIF) 32
3.5.1 Megascopic Description 33
3.5.2 Microscopic Description 33
3.6.1 Megascopic Description 36
3.6.2 Microscopic Description 36
3.7 GREENSTONE 38
3.7.1 Megascopic Description 38
3.7.2 Microscopic Description 38
3.8.1 Megascopic Description 40
3.8.2 Microscopic Description 40
3.9. 1 Megascopic description 42
3.10 MEDIUM GRAINED BIOTITE GRANITE 43
3.10.1 Megascopic Description 44
3.10.2 Microscopic description 45
3.11 PORPHYRITIC GRANITE 46
3.11.1 Megascopic Description 46
3.11.2 Microscopic Description 47
3.12.1 Joints 48
3.12.2 Foliations 49
3.12.3 Faults 50
3.12.4 Fold 52
CHAPTER 4 53
GEOCHEMISTRY 53
4.1 SAMPLING AND ANALYTICAL TECHNIQUES 53
4.2 RESULTS 53

4.3.2 Trace elements composition 62
4.3.3 Lithophile Element Distribution Pattern 62
4.3.4 Origin of the Iron-formations (The BIF) 63
CHAPTER 5 67
MINERALISATION POTENTIAL OF THE STUDY AREA 67
5.1 PREAMBLE 67
5.2 GOLD 67
5.4 POTENTIAL SITE FOR OTHER MINERALS 73
CHAPTER 6 74
SUMMARY, CONCLUSION AND RECOMMENDATION 74
6.1 SUMMARY 74
6.2 CONCLUSION 75
6.3 RECOMMENDATION 75

LIST OF FIGURES

Figure 1.1: Location map of the study area. .....**Error! Bookmark not defined.**

Figure 1.2: Map of the drainage pattern of the study area 5

Figure 2.1: Schist belt localities within the context of the Geology of Nigeria (After Woakes et al., ... 18

Figure 2.2: Regional geology of the northwestern Nigeria Pan-African terrain (after Ball 1980, Danbatta, 2003) 19

Figure3.2:Rose diagram for the study area.……48

Figure 4.1: TiO2 versus SiO2 discrimination diagram (Tarnrey, 1977). Line separates sedimentary from igneous rocks……..58

Figure 4.2: MnO/FeOtot- diagram (wt %), (Mücke 2005) BIF sample in the study area showing the manganese formation and iron-formation area..... 60

Figure 4.3: Fe-Mn-(Co+Ni+Cu+Zn)*10- diagram to differentiate submarine hydrothermal and hydrogenous deposit (Bonatti et al., 1972) and the analytical plot of the BIF in the study area……..…..63

Figure 4.4: A ternary plot of SiO_2; (FeO+MnO); Fe_2O_3 of the BIF in the study area (After Mucke, 2005)……64

Figure 5.1: Mineral map of the study area……..85

LIST OF TABLES

Table 1: A generalized geochronology for the basement rocks of Nigeria (modified after McCurry, 1976; Dada, 1997)……17

Table 2: Major elements compositions of rocks from the study area (Wt%)……..54

Table 3: Calculated total elemental iron and manganese of the BIF (Wt%) …….55

Table 4: Trace elements compositions of rocks from the study area (ppm) ……..…55

Table 5: Lithophile elements composition (ppm) ……...56

Table 6: Lithophile element ratios ……..56

LIST OF PLATES

Plate I: An extensive ridge of the granitic gneiss at Kwatarkwashi ….. 24
Plate II: Conspicuous mineralogical banding of the granitic gneiss revealing the gneissic structure. 25
Plate III: Joints trends on the granite gneiss 25
Plate IV: Medium grained texture of the granitic gneiss rock with quartz vein..... 26
Plate V: Photomicrograph of granitic gneiss under PPL and XPL, Mg x 10. ..... .27
Plate VI: Photomicrograph of gneiss under PPL and XPL displying foliation trend, Mgx10.....29
Plate VII: Photomicrograph of Biotite-muscovite schist under PPL and XPL displaying the foliated biotite crystals……30
Plate VIII: Metasedimentary ridge containing the BIF extending for about 40Km N-S 31
Plate IX: Reddish brown BIF with various boulders displaying the banding(B) 32
Plate X: Photomicrograph of the BIF block slide from the study area under reflected light, Mg x 30 33
Plate XI: Photomicrograph of the BIF slide from the study area, Mg x30……. ..…..34
Plate XII: Photograph of the dome shape of the hornfels outcrop..... 35
Plate XIII: Photograph of Quartz vein trending 068^{o} within the hornfels……..……35
Plate XIV: Photomicrograph of the hornfels under PPL, Mg x 10..... 37
Plate XV: Photomicrograph of the greenston under PPL and XPL, Mg x10..... 38
Plate XVI: Photomicrograph of the granodiorite under PPL and XPL, Mg x10..... 40
Plate XVII: Photograph exposure of Medium grained biotite granite at Chafe 42
Plate XVIII: Photograph of boulders at the foot of the granite located at Chafe and Magazu 43
Plate XIX: Joints on granite at Chafe..... 44
Plate XX: Photomicrograph of the medium grained biotite graniteat Chafe, under PPL and XPL, Mg x10 45
Plate XXI: Porphyritic texture at some parts of Chafe granite.....……46
Plate XXII: Photomicrograph of Porphyritic granite under PPL and XPL, Mg x10..... 47
Plate XXIII: Photograph of cross cutting joint trend on the grantic-gneiss 49

Plate XXIV: Phyllite exhibiting NE-SW foliation trend in the study area 50
Plate XXV : Faulted aplite dyke in a Diorite in the study area 51
Plate XXVI : Simple assymetrical fold on muscovite-schist 52
Plate XXVII :Photograph showing the amount of gold won in every full of pan washed using the local sluice machine……66
Plate XXVIII**:** Artisanal miners using a local sluice box machine to sieve the gold from the alluvium……67
Plate XXIX: Artisanal miner using the local pan to wash the gold in River Gajere…….67
Plate XXX : Artisanal miners carrying their local tools for their artisanal gold mining activities…….68

LIST OF APPENDICES

APPENDIX A 79
APPENDIX B 81
APPENDIXC…. 82

CHAPTER 1

GENERAL INTRODUCTION

1.1 DEFINITIONS

Mineral resource potential is the likelihood for occurrence of undiscovered mineral resources in a defined area. It is closely related to mineral resource favorability. The term "resource potential" is a preferred term for the description of an area while "resource favorability" is preferred for description of a specific rock mass or geologic environment Tailor and Steven, (1984) (nwrc.usgs.gov/techrpt/sta13pdf.)

Low potential is assigned to areas where geologic, geochemical, and geophysical characteristics define environments in which the existence of resources is unlikely. This broad category embraces areas that have dispersed but insignificantly mineralized rock, as well as areas that have few or no indications of being mineralized.

Moderate potential is assigned to the following areas (a) where; geologic, geochemical, and geophysical characteristics indicate environments favorable for resource occurrence; (b) interpretations of data indicate a reasonable likelihood of resource accumulation, and (c) application of knowledge of types of mineral deposits indicates favorable ground for specific types of deposits.

High potential is assigned to areas where: (a) geologic, geochemical, and geophysical characteristics indicate environments favorable for resource occurrence; (b) where interpretations of data indicate a high degree of likelihood for resource accumulation; (c) where knowledge of types of mineral deposits supports determinations of the presence of resources, and (d) where data

indicate that minerals have concentrated in at least a part of the area. Resources or deposits need not to be identified for an area to have high resource potential (Tailor and Steven (1984) (nwrc.usgs.gov/techrpt/sta13pdf,).

Unknown potential is assigned to areas where information is inadequate to assign low, moderate, or high levels of potential. This category is generally used for areas that have covering rock units and have inadequate geophysical and geochemical data. The phrase "no potential" should be applied only to a specific kind of resource in a carefully defined area; it should not be used as a summary rating for all commodities in any area.

1.2 LOCATION AND ACCESSIBILTY

The study area lies within the Northern part of Wonaka Schist belt, northwestern Nigeria (Fig. 1). The study area is bounded by Latitudes 12^{o} 15' 00"N and 11^{o} 53' 00"N and Longitudes 06^{o} 45' 00"E and 7^{o} 00' 00"E within Sheet 54 (Gusau) and Chafe Sheet 77. It covers an area of 1090 km^{2}. It is about 12.5 km South of Kwatarkwashi town. The area is accessible by foot paths, tarred and un-tarred roads from Kwatarkwashi, Mada and Chafe towns. These three towns are linked by a major road from Funtua to Gusau, the State capital of Zamfara State. There is a rail line from Kaura-Namoda to Kano through Chafe. Footpaths and cattle tracks are widespread, joining homes and farm lands.

1.3 RELIEF AND DRAINAGE

Relief in the study area is slightly higher in the northwestern and south- eastern parts of the study area as compared to the north- eastern and southwestern part. The landform is generally flat but at the North western and South eastern part of the study area are Kwatarkwashi and Chafe with the highest relief of about 2200 m above mean sea level on the Kwatarkwashi ridge and Chafe hills. The metasedimentary ridge in the study area has a high relief of 1950 m above mean sea level at Biya-Buki (Fig. 2). The extreme North- eastern part has the lowest relief of about 1350 m above mean sea level at Koha village.

The drainage pattern is dendritic and is defined by rivers Mada, Sokoto and Gajere which are the major rivers in the area. The Sokoto and Gajere rivers flow almost in the same direction SE- NW at the SW and NE quadrants respectively. River Mada and its tributaries drain into Butsa to Fura-Girke which all flow in to river Gajere, while the Kauye-Jatau, Dan-Ladan and Tubuibui streams are all tributaries of the Sokoto river. The study area is well drained such that most of the streams and Gajere and Sokoto Rivers are seasonal and only flow during the rainy season (Fig. 3)

1.4 CLIMATE, VEGETATION AND LAND USE

The study area lies within the warm tropical region with an annual temperature rising up to 38^{o} C between March to May. The rainy season is from May to September, the highest amount of rainfall is recorded in August, while the cold season known as Harmattan lasts from December to February.

December to February is a period of dryness, with little or no precipitation, which is accompanied by harsh, dry northeasterly wind that is often laden with dust from the Sahara and result to low humidity.

Vegetation in the area is typical of Guinea savannah just like in other parts of the country where this biome occurs, it is characterized by woodlands, where grasses occur either totally or mixed with other herbaceous or shrubby plants. The grasses are green in the wet season with fresh leaves, but become dry during the dry season when bush burning, fire wood cutting and other human activities take place. The districts are mainly inhabited by peasant farmers that grow maize, guinea corn, rice and groundnuts during the rainy season. In the dry season, most of the inhabitants graze their animals, while others turn to major rivers and engage into gold panning.

1.5 PREVIOUS WORK

The earliest work on the belt was by McCurry, 1973 who reported that the belt is situated Northwest of Karaukarau belt with a major foliation and N-S rock orientation trend. The work showed that petrographically, Wonaka schist belt is composed of fine grained quartz-biotite rocks in some places containing sillimanite, cordierite or garnet. Thin beds of calc-silicate rocks are

widely distributed in the west, biotite- muscovite schist, quartzites, ferruginous schist, gneisses and mylonites are equally present.

According to (McCurry, 1973), metamorphism in Wonaka schist is of higher temperature and lower pressure type than in other schist belt. This could be due to the close association with large batholithic masses of granite and granodiorite which almost engulf to the Wonaka schist belt.

Harper et al., (1973) revealed that Wonaka and Karau-karau schist belts have similar geochronology. K-Ar ages for whole rocks and biotite range from 515 to 550 Ma and represents cooling ages at Karau-karau.

Turner (1983), reported that the rocks of Wonaka schist belt are mudstones and marls; traversing westward of Kazaure belt, through the Karau-karau to the Wonaka belt, the amount of course grained clastics is progressively reduced. The three belts may, therefore, contain different facies of one sedimentary basin, and so the Wonaka schist belt is also provisionally assigned to the Pan-African.

According to Woakes and Bafor, (1984), suggested that primary gold deposits are associated with some schist belts (e.g. Ilesha, Maru, Anka, Kushaka) and not with others (Wonaka, Karau-karau, Iseyi-Ogun River), and that they are often spatially related to amphibolites and regional NE-SW to N-S fault or shear zones, with no specific relationship or BIF.

1.6 AIM AND OBJECTIVES OF PRESENT WORK

This research project is aimed at studying the geology, geochemistry of rocks and banded iron formation of the northern part of Wonaka schist belt. Therefore the scope of the research involves a comprehensive geological, structural and geochemical study of northern part of Wonaka schist belt, with a view to:

a) Produce a detailed geological and mineral maps of the study area on a scale of 1:50 000.

b) Undertake petrographic study of the component rock types.

c) Provide mineral and chemical data through geochemical analyses of representative samples that are systematically collected from the area.

d) Determine the geology and geochemistry rocks and banded iron formation of northern part of Wonaka schist belt.

1.7 RESEARCH METHODOLOGY

1.7.1 Field Mapping

Field mapping was carried out on a scale of 1:50,000, using a planumetric map extracted from Sheet 8 (Gusau) and Sheet 77 (Chafe). The field mapping was accomplished by selected traverses and use of field equipment such as Global positioning system (GPS) and compass clinometer etc.

The mapping was done in four stages beginning from a reconnaissance survey for the purpose of familiarization with ground attributes of geologic features and to select access routes to reach outcrops identified from Google Earth map. Subsequent visit were carried out in January, April, and May 2012 for detailed mapping.

Map from Google Earth was very useful map used for mapping. It was a useful guide in the general interpretation of features and structures.

1.7.2 Sampling and Sample Preparation

In all, nineteen samples were collected out of which one was a soil sediment. Sampling interval for the rock samples varied depending on the aerial extent of each outcrop and field environmental conditions encountered. These samples cover mainly granitic-gneiss, gneiss, hornfels, schist,

granites, greenstone, banded iron formation, granaodiorites, diorite, with poorly expose pegmatites. The samples were crushed and pulverized into fine powder at Department of Geology, Ahmadu Bello University, Zaria. Thin sections of rock sample and polished sections of the banded iron formation of rock samples were also made in the Department of Geology.

A total of fifteen samples were taken to Department of Geology , Kano University of Science and Technology, Wudil for whole rock geochemical analysis using XRF technique as well as Center for Energy Research and Training (CERT), Ahmadu Bello University Zaria for Flame Photometry technique to determine alkalis concentrations of the samples.

.

1.7.3 X-Ray Fluorescence (XRF)

This technique is chosen because it is a non-destructive analytical technique used to identify and determine the concentrations of elements present in solid, powdered and liquid samples. XRF is capable of measuring elements from Beryllium (Be) to Uranium (U) at trace levels and up to 100%. It is the most widely used analytical technique in the determination of the major and trace element chemistry of rock samples (Rollinson, 1993). It is based on the formation of fluorescence as result of the quantum energy released when an atom is de-exited after irradiation with X-rays. The X-ray photons are a form of electromagnetic radiations (10 -100 ev range of energy). They are produced when high speed electrons decelerate or when electron transition occur involving inner orbit energy state of atoms.

When any sample is bombarded with electron radiation (irradiation), an inner shell electron is ejected, which leaves the atom in an excited state. A de-excitation process occurs to return it to a

stable ground state. The vacancy created by the emission of an inner shell electron is filled by an electron previously residing at a higher energy level. The excess energy resulting from the transition is often dissipated as electromagnetic radiation called x-ray photon.

These photons have a very narrow energy band-width and are specific for particular electro transition that occurred and are characteristic of the elements from which they are emitted. The x-ray that is emitted by the sample are absorbed by the detector which act as diode in converting these incident x-rays to electronic pulses whose amplitudes are proportional to the energies of the corresponding x-rays. The pulses are processed and sorted according to the amplitude. The entire range of pulses amplitude is divided into 1024 intervals called channels and those pulses falling within each interval are counted in a multi-channel analyzer. The channel number is usually converted into units by calibrations. The intensity or number of counts in a peak is a direct result of the number of fluorescing atoms of that element in the sample. Thus, the area under a peak is proportional to the concentration of that element in the sample.

1.7.4 Flame Photometry

Flame photometry technique method was employed in addition to the XRF analytical method initially employed to determine the concentration of Na in the samples that was not determined by XRF probably due to technical specification limit of the machine.

Flame photometry is one method in the general field of emission spectroscopy. The flame photometry is especially useful in the determination of an alkali and similar metals because of the scarcity of other good quantitative methods for these substances. The flame is especially useful because of its simplicity for routine analyses which are difficult by other means. Thus, the alkali

metals with their low excitation energies are easily determined with this method, while they are difficult to do by other means.

The atomizer was carefully cleaned to check contamination. It was accomplished by atomizing distilled water through the system with the flame operating.

Next the instrument was turned on and allowed to warm up for 15 to 30 min with the flame on to allow approximate establishment of a thermal steady state. The operator supplied additional operating instructions and precautions for the particular instrument used.

A working curve for sodium ion was determined using the direct-intensity method. A standard sodium ion solution was used to set the 0% T with distilled water and the 100% T with the 100-µg/ml solution. Without changing the slit settings, the % T for the other concentrations was determined. A proper wavelength was set on the instrument for sodium ion (589 nm) before any measurements was carried out. (For potassium ion, a wavelength of 767 nm was used.)

25 ml of the prepared sample solution was pipetted into a 100-ml volumetric flask, diluted to the 100 ml mark and mixed thoroughly. This diluted sample was measured on the flame photometer at the same time the direct-intensity working curve was prepared using the same instrument settings.

To determine the data for a working curve of sodium ion, the internal-standard method was used. The standard sodium ion solutions which contain 100 µg/ml lithium ion; set the 0% T with the 0-µg/ml sodium ion solution and the 100*%T* with the 100-µg/ml sodium ion solution. Using the slit settings for the 100-µg/ml solution the relative *%T* for sodium and lithium was determined. A wavelength of 671 nm for lithium ion measurements was used.

25 ml of the of the prepared sample solution was pipeted into a 100-ml volumetric flask; then 10 ml of the lithium stock solution (1000 µg/ml) was pipeted into the 100-ml volumetric flask; diluted to the 100 ml mark and mixed thoroughly. The diluted sample on the flame photometer was

measured at the same time the internal-standard working curve was prepared using the same instrument settings.

The importance of scrupulous cleanliness was emphasized by (*a*) dipping two fingers into 20 ml distilled water and measuring the resulting sodium ion concentration on the flame photometer (using the direct-intensity method), (*b*) measuring the sodium ion content of tap water, and (*c*) measuring the sodium content of various regents which are not supposed to contain sodium ion. A correction for the latter effect was taken care of by carrying out a "blank" determination.

Flame photometry has many disadvantages. Perhaps the most difficult of these is the control of the many variables. The intensity from a flame is dependent on the flame temperature, the rate of flow of liquid into the flame, the pressure and rate of flow of fuel gases, and any of many other variables which affect the character of the flame or atomizing of the solution have a great effect. The experimental results are therefore only empirical.

The spectrum obtained with the flame is due to the following order of events. The solution of the metal salt in question was sprayed into the flame and the solvent evaporated leaving the finely powdered salt. The salt is vaporized, atomized, and a valence electron is raised to a higher-energy state. The energy emitted when this electron drops down into a vacant lower level is given off as radiant energy of a wavelength determined by the Planck-Einstein relationship:

$$\Delta E = h\nu = \frac{Hc}{\Lambda}$$

Where h = Planck's constant

c = velocity of light

v = frequency of light emitted

λ = wavelength

The change in energy corresponding to light of wavelength 500 nm is

$$\Delta E = \frac{6.6 \times 10^{-27} erg \cdot s \times 3 \times 10^{10} cm/s}{500 \times 10^{-7} cm} = 3.96 \times 10^{-12} ergs$$

CHAPTER 2

REGIONAL GEOLOGY

2.1 THE BASEMENT COMPLEX OF NIGERIA

The basement complex of Nigeria lies in a vast area east of the West African Craton that was subjected to the Pan-African orogenic event about 600 Ma ago. Evidence from Hoggar (Pharusian), Ghana and Togo indicates that this belt evolved through plate tectonic activities involving collision and subduction resulting in the partial melting of the lower crust and formation of granitic magma leading to the emplacement of the Older Granites (Ajibade and Wright, 1989).

Within the basement are domains of metasedimentary, metavolcanics and intrusive igneous rocks which constitute the north-south trending schist belts. They are considered to be Upper Proterozoic assemblages that lie on the migmatites-gneisses-quarzite complex (Turner, 1983). The schist belts which are concentrated in the western half of Nigeria are seldom found east of 8^0 E longitude (Ajibade and Wright, 1989; Akintola and Adekeye, 2008). They host most of the economic minerals in the basement complex (Akande and Kinnaird, 1990). The following rock groups are recognized in the Nigerian Basement Complex;

Polycyclic migmatites-gneiss-quartzite complex

Schist belts composed of metasdimentary and metavolcanics

Older Granites and

Minor felsic and minor intrusive.

2.2.1 The Migmatites-gneiss-quartzite complex

The migmatites-gneiss-quartzite complex are high grade metamorphic rocks of various compositions which are believed to account for about 60% of the basement rocks of Nigeria (Rahaman et al., 1988). They usually comprise of migmatite and gneiss of various composition and structures. Metamorphism is generally in the amphibolites to granulite facie grade. Associated with these are relicts of ancient metasediments (commonly feldspathic quartzites) which were correlated with the Birrimian metasediments of Ghana McCurry (1976). The gneisses and migmatites are so intimately associated such that they are hardly separated in the field. They are commonly seen and form the bulk of the rocks in this group. Banding of various widths is the common feature or structure displayed by these rocks.

According to Dada (1997), there was crustal addition in the crystalline basement complex of Nigeria that occurred about 3500 Ma. Dada obtained ages greater than 3000 Ma from some of the basement rocks as shown in a geochronology for the basement rocks of Nigeria modified by Dada (1997) after McCurry (1976). Age determination across the country shows that the migmatite-gneiss complex contains rocks that are as old as 3000 Ma and those as young as 600 Ma as shown in Table 1.

Table 1: A generalized geochronology for the basement rocks of Nigeria (modified after McCurry, 1976; Dada, 1997)

Age (Ma)	**Period (or epoch)**	***Activity***	***Remarks***
540 ± 40	Late Pan – African	Uplift, cooling, faulting, high level magmatic activity	
650 – 580	Pan – African	Granitic intrusion, pegmatites and aplite development	Older Granites Magmatism
650 – 850	(Main phase)	Orogenesis: deformation, metamorphism, migmatisation and reactivation of pre – existing rocks	
800 – 1000	Katangan	Geosynclinal deposition, intrusion of hypersthenes – bearing rocks.	Katangan Metasediments
1900 ± 250	Eburnean	Granite intrusion Orogenesis: folding, metamorphism and reactivation of pre – existing rocks.	Eburnean granites
2500	Birrimian	Geosynclinal deposition	Birrimian metasediments
3100 – 2750 Dada (1997)		Orogenesis and metamorphism	Emplacement of granodioritic magma
3500 Dada (1997)		Crystalline basement	Crustal addition

Ajibade and Wright (1989), accumulating field evidence, particularly from Minna area, reported that parts of the basement were formed as a result of magmatic injection into low grade schist belts.

2.2.2 Schist Belts

The schist belts form approximately north to south trending narrow zones of low to medium grade metamorphic rocks of mainly sedimentary and minor igneous origin, which were deposited previously on the pre-existing migmatite- gneiss-quartzite complex. The rocks of the belt are also described as 'Younger Metasediments' composed of phyllite, schist quartzite, amphibolites and flaggy gneiss of Paleo-Proterozoic age (Akande and Kinnaird, 1990). Other secondary rocks used in delineating them are carbonates, calc-gneiss and Banded iron formation (BIF). Metamorphism within the schist belts is predominantly of the greenschist facies grading into the amphibolites facies, especially in the older migmatite-gneiss-quartzite complex (Akande and Kinnaird, 1990).

About ten schist belts have been described and named in northwestern Nigeria (Fig. 2.1), which include;

1) Zuru (2) Anka (3) Maru (4) Wonaka (5) Kazaure (6) Karaukarau (7) Kushaka (8) Zungeru-Birnin-Gwari (9) Malumfashi and (10) Kusheriki.

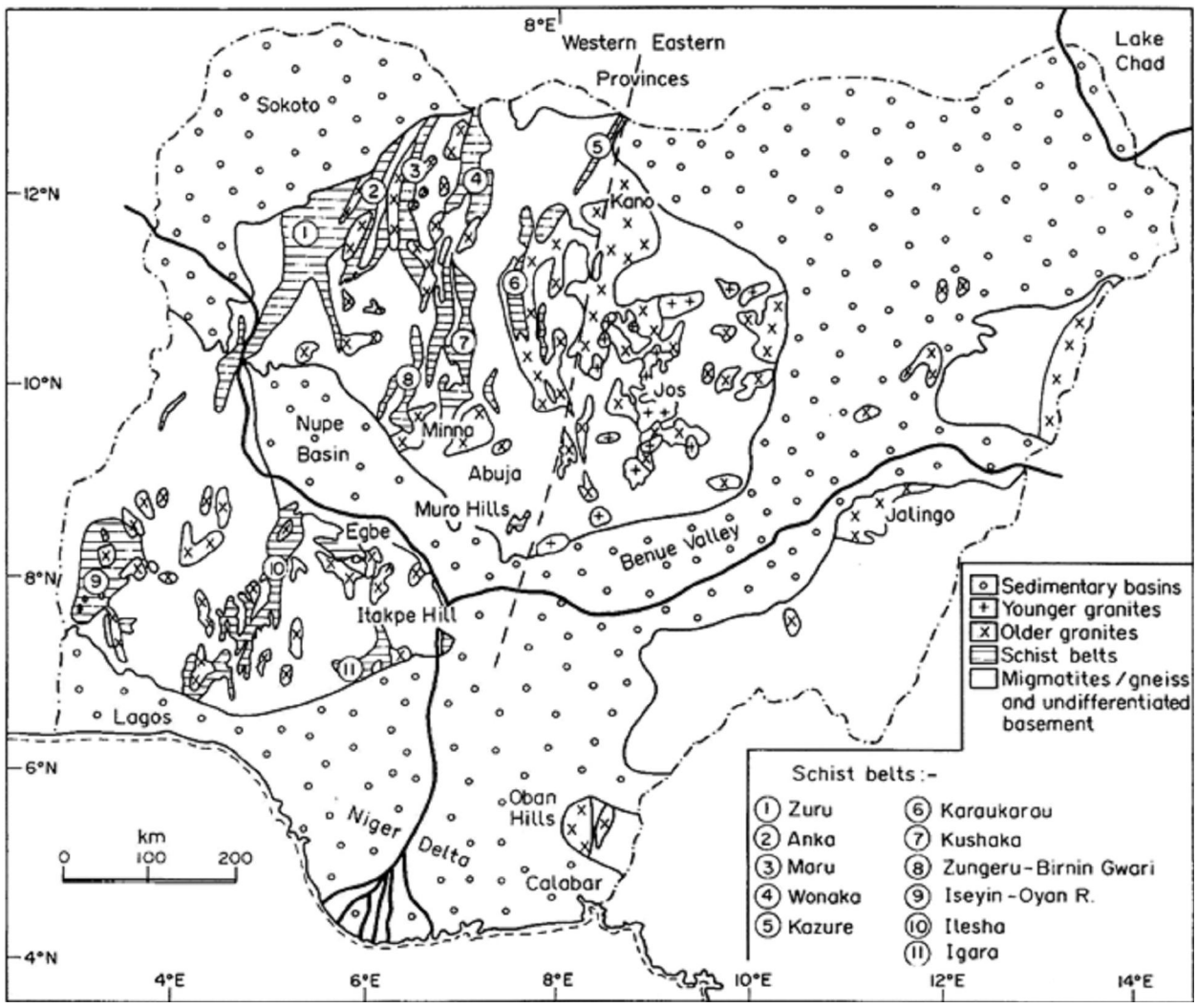


Figure 2.1: Schist belt localities within the context of the Geology of Nigeria (After Woakes et al., 1983**).**

Structurally, two major transcurrent fault systems with dextral displacements are known in the Precambrian basement. They trend in the NE-SW direction displacing earlier structures in the order of tens of kilometers. The two fault systems are the Anka fault and the Kalangai fault (Fig. 2.2) and are often associated with locally developed subsidiary (NW-SE) sinistral fault and are

considered to be conjugate system of late Pan-African brittle deformation that occurred after about 530 Ma on a continental scale (Ball, 1980; Danbatta, 2003b).

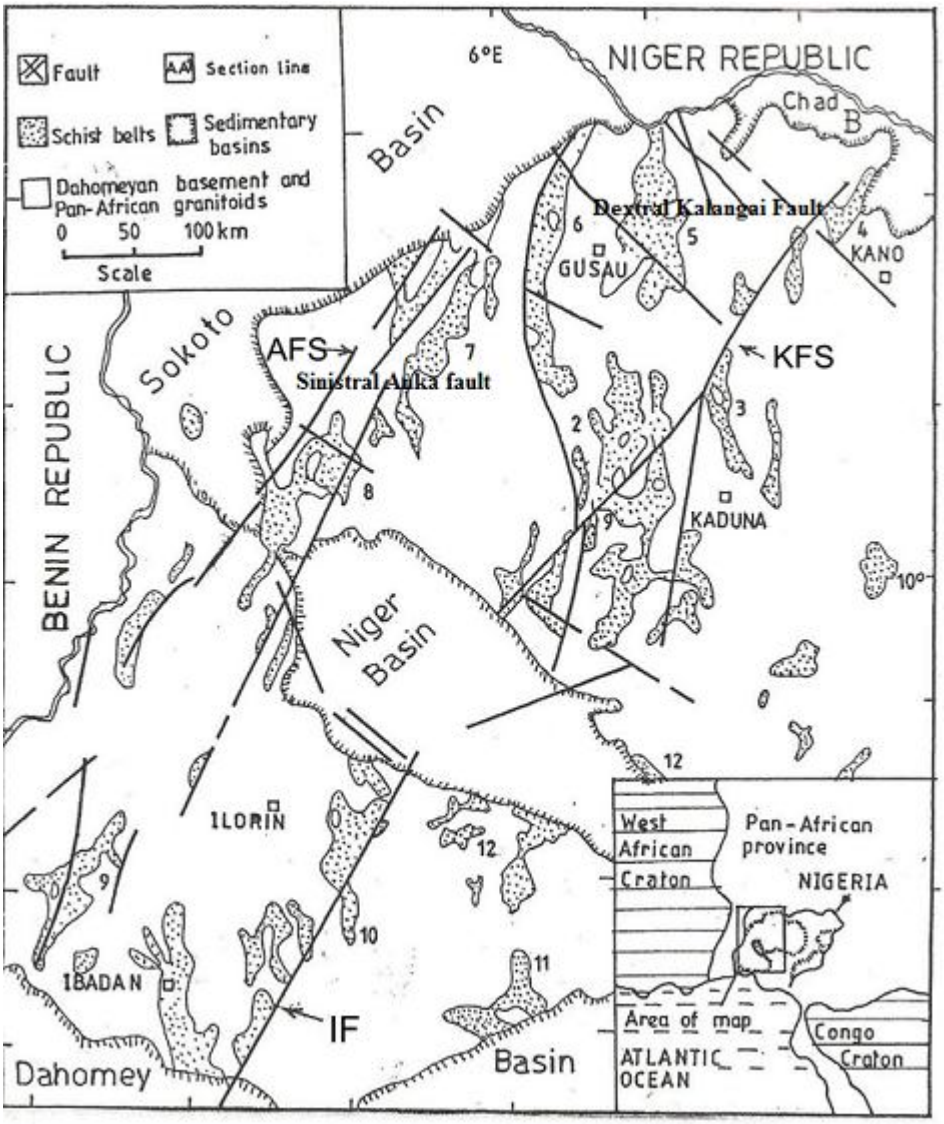


Figure 2.2: Regional geology of the northwestern Nigeria Pan-African terrain showing the dextral Kalangai and sinistral Anka faults system in NW-SE and NE-SW directions cutting across Wonaka and Anka schist belts respectively (after Ball, 1980; Danbatta, 2003**)**

The mineral resource associated with some of the northwestern schist belts include gold in Zungeru-Birnin Gwari, Wonaka, Kushaka and Anka belt; iron ore in Maru, Wonaka, serpentine in

Tungar Kudaku and Malam Tanko all in Anka schist belt as well as clay in almost all the schist belts(Danbatta, 2003).

2.2.3 The Older Granites

These intrude the migmatite-gneiss complex and low grade schist belts. In general, the Older Granites range in size from sub-elliptical plutons to elongated batholiths up to 60 km. The bodies are usually elongated parallel to the regional trend and may be foliated. Foliation when present is also parallel to that of the country rocks. The Older Granites vary in composition from true granites to granodiorites and tonalities. They also vary in texture from fine grained to coarse grained porphyritic granites rocks. However, the medium to coarse-grained porphyritic variety is more common. Other rock types which normally occur in association with granitic rocks include charnockite, gabbro and syenite. One striking feature of Older Granite is their picturesque inselbergs such as Kufena Hill in Zaria, Zuma rock in Suleja, Olumo Rock in Abeokuta, Idanre Hills in Idanre and Ikere Hills in Ikere Ekiti (Olayinka, 2009).

Field relations show that Older Granites are composite bodies, usually composed of two or more intrusions. Several workers such as Trustwell and Cope, (1963), Mccurry and Wright (1971), and Danbatta (1999) carried out a detailed work in Northwestern Nigeria and all classified the Older Granites into syntectonic granites. These authors believed that the granites were partly intrusive and partly metasomatic. The late tectonic granites are fine grained, aplitic or dioritic which clearly cross-cut the syntectonic granite.

2.2.4 Minor Felsic and Mafic Intrusives

The minor felsic and mafic intrusives consist of concordant and discordant dykes, veins and irregular bodies of pegmatite, aplite, quartz, dolerite, gabbro, pyroxenite and serpentinite. As the

youngest members of the basement complex of Nigeria, rocks of these units intruded almost all the pre-existing rocks. The pegmatite host tourmaline and beryl gemstones, tantalite, columbite and cassiterite. They also contain feldspars and micas in exploitable quantities.

.

.

CHAPTER 3

FIELD GEOLOGY AND PETROGRAPHY

3.1 INTRODUCTION

The study area falls within the Wonaka schist belt and comprises of the following major rock types; granitic gneiss, gneisses, metasedimentary rocks and granite while aplite dykes and pegmatites occur as minor rocks that all make up the lithologic units of the belt.

3.2 GRANITIC- GNEISS

The granitic-gneiss is exposed at Kwatarkoshi town, close to the main road leading to Gusau town, the State capital of Zamfara State. It belongs to the Migmatite-gneiss- quartzite complex of the north-western Nigeria and is an elevated ridge with an average altitude of about 2100 metres (Plate I). It is situated at the northern and western part of the town (Fig. 2), with a general NNE-SSW trend and a conspicuous banding (Plate II) that trends N-S. The colour of the rock varies from grey to pink from place to place. The rock body extends up to the end of the eastern boundary of the study area, where it is bounded by a granodiorite at the northeastern part of the study area around Butsa. To the east, it is bounded by a diorite around Mada town and to the south, it is in contact with the schist rock in the area (Fig. 2).

At the top of ridge, the composition of the rock is granitic, while the lower parts of the ridge are gneissic in composition. Some structural features such as quartz veins, joints, foliation etc are present. Quartz veins are of various sizes ranging from 27cm wide and 20m long (Plate IV) with N-S orientation. The texture of the rock varies from fine-grained, medium-grained to porphyritic.



Plate I: An extensive ridge of the granitic-gneiss at Kwatarkwashi.

Note the extension of the exposure on the plate I at the left hand side of the Funtua-Gusau road occurring as low-lying whaleback



Plate II: Conspicuous mineralogical banding of the granitic-gneiss revealing the gneissic structure as well as the grey colour of the rock**.**



Plate III: Joints trends on the granitic gneiss at Kwatarkwashi.

3.2.1 Megascopic Description

The rock is grey in colour and porphyroblastic with distinct megacryst of feldspars and quartz. The quartz grains ranges in size from 2 to 5 cm and are aligned in a N-S direction. The rock is banded in hand specimen. The conspicuous alignment of mafic minerals and that of the feldspars gives it a gneissic texture. The minerals observed in hand specimen are biotite, quartz and feldspars.

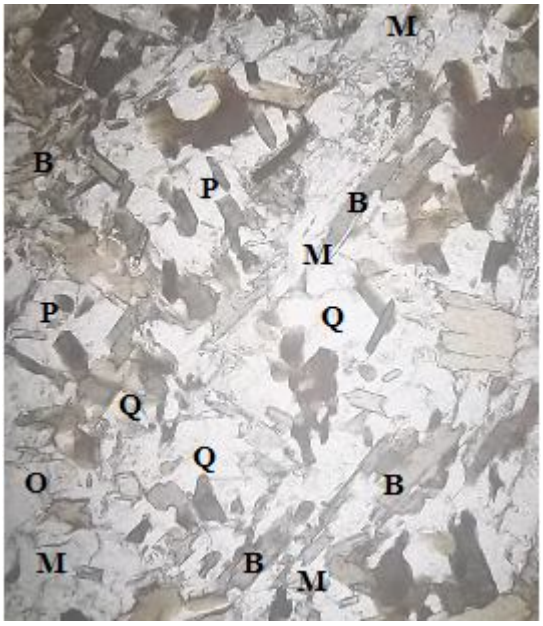


Plate IV: Medium grained texture of the granitic gneiss rock with quartz vein.

3.2.2 Microscopic Description

Sample examined under the microscope show a kind of preferred orientation of almost all the minerals in a specific direction. The rock is generally course grained in texture with quartz as the most abundant mineral (about 40%). The quartz is subhedral and colourless in colour with the

characteristic wavy extinction. Biotite crystals are brown in colour with its distinct one directional cleavage (Plate v). The biotite constitutes about 35% of the rock. Appreciable amounts of plagioclse feldspars about 20% are present, with little orthoclase feldspars and muscovites.

(a) 

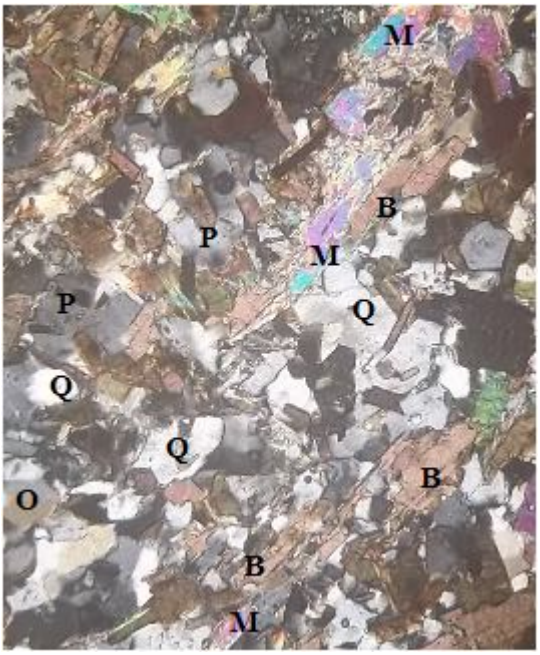
(b) 

Plate V; Photomicrograph of granitic gneiss (a) under PPL and (b) under XPL B - Biotite, M-Muscovite, Q-Quartz, P-Plagioclase feldspars, O-Orthoclase feldspars. Mg x10

3.3 GNEISS

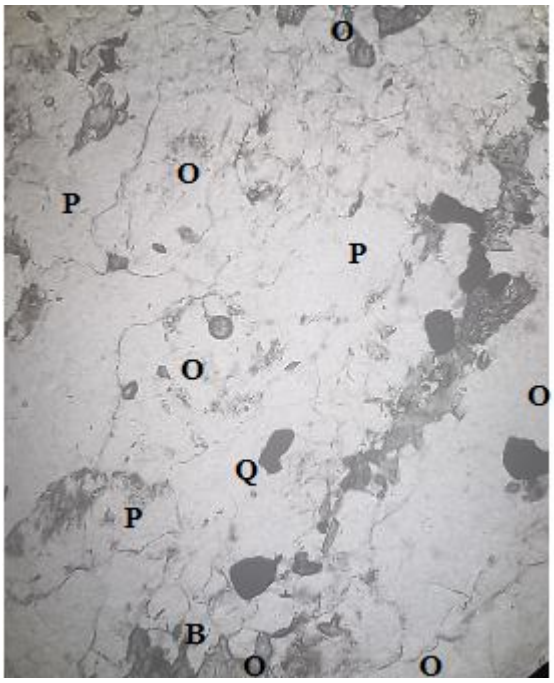
The gneiss outcrops is about 2 km west of Mada town. It is situated east of the granitic gneiss at Kwatarkwashi. It is a well exposed outcrop that occurs in boulders form. It is light coloured with NE-SW orientation. The gneiss makes a boundary with the medium grained granite to the south east, diorite to the north east and the schist to the south west (Fig. 2), it is the eastern extension of the Gusau migmatite-gneiss complex.

3.3.1 Megascopic Description

The gneiss is banded in hand specimen displaying preferred orientation of mica crystals. The rock is composed of pink orthoclase feldspars as the most abundant mineral of the rock, thus, gives the rock a pink colour. Quartz and dark coloured minerals are also present. The rock has a fine grained texture,

3.3.2 Microscopic Description

Sample of the rock examined under the plane polarized light shows that the rock is foliated, containing orthoclase feldspar as colourless crystals exhibiting Carslbad twinning and the most abundant mineral of the rock, up to about 45% (visual estimation). The biotite is brown to green in colour with straight extinction. The biotite displayed distinct one directional cleavage. It constitutes about 35% of the rock. Plagioclase feldspar is present about 10% (visual estimation). Quartz crystals are equally present, about 10% of the rock (Plate VI).

(a) 

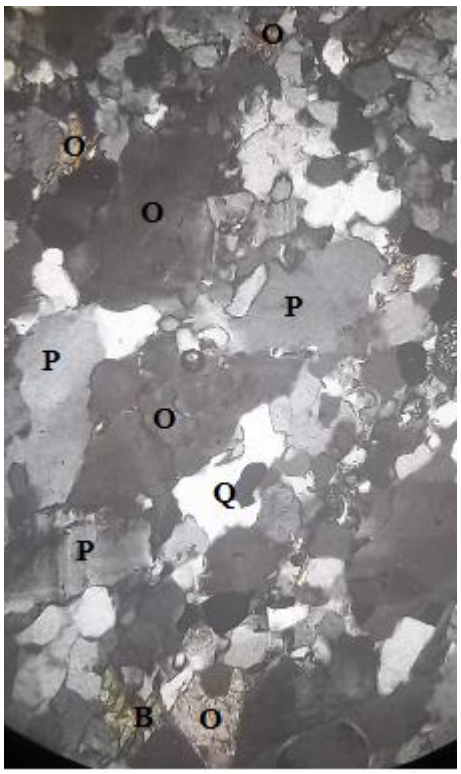
(b) 

Plate VI: Photomicrograph of the gneiss (a) under PPL and (b) displaying it foliation trend. O- Orthoclase feldspar B - Biotite, P - Plagioclase feldspar, Q – Quartz. MG X10.

3.4 BIOTITE- MUSCOVITE SCHIST

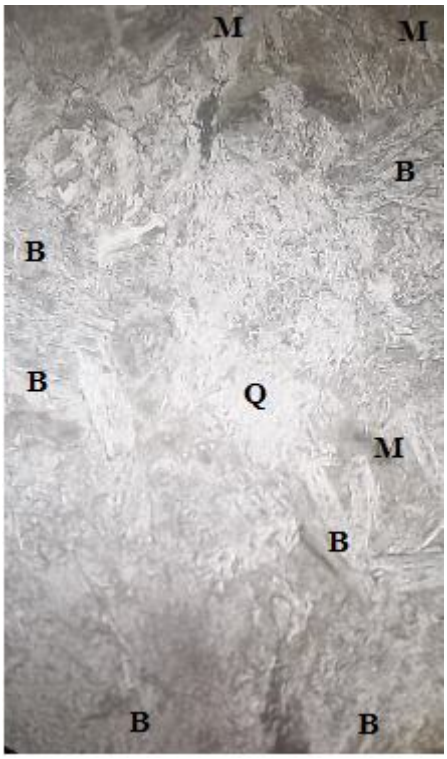
It is dark brown in colour and foliated. The schist is composed of silicified muscovite schist interbedded with thin layers of carbonaceous schist. It trends in a N-S direction.

3.4.1 Megascopic Description

The rock MA4 examined on hand specimen is a dark coloured rock with a clear whitish bands round the sample but not alternating. It is composed of high amount of shiny feldspars crystals and dark coloured mica crystals. The rock is very fine-grained.

3.4.2 Microscopic Description

The rock examined under the microscope is foliated and mainly characterized by the biotite crystals. The biotite is brown with straight extinction and one directional cleavage. It is about 60% of the rock (visual estimation). Muscovite is also present up to about 25% of the rock (visual estimation). Quartz colourless crystal with distinct wavy extinction is equally present occur in a very minute quantity, about 5% of the rock composition, (Plate VII).

(a) 

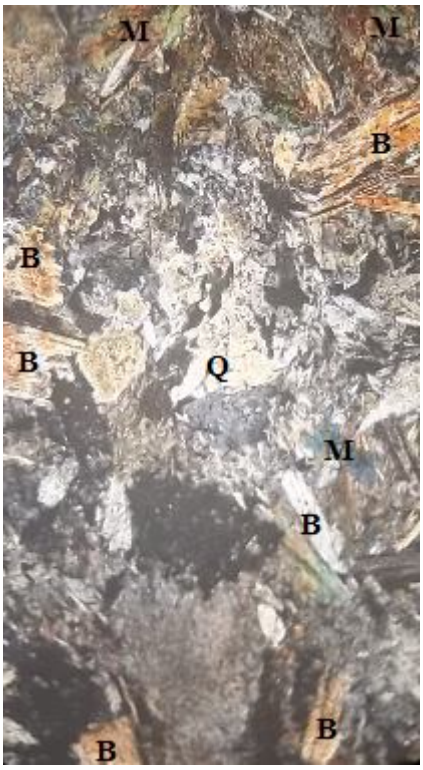
(b) 

Plate VII; Photomicrograph of biotite muscovite schist under (a) PPL and (b) XPL
B - Biotite, M- Muscovite, Q-Quartz. Mg x10

.

3.5 THE BANDED IRON FORMATION (BIF)

In the central parts of the study area, is a N-S trending large and extensive ferruginized metasedimentary ridge containing Banded iron formation (Plate VIII).



Plate VIII: The metasedimentary ridge extending for about 40km in a N-S direction.

The metasedimentary ridge is composed of schists and phyllites interlayered with BIF. The BIF forms the ‘‘spine of the ridge’’. The BIF is highly weathered and well exposed on the metasedimentary ridge with an altitude of about 1800 meters (Fig. 2). At the foot of the metasedimentary ridge is large deposit of laterite observed within a dry stream channel.

At $11^{o}\,57'\,08''$N and $006^{o}\,53'\,46''$E, five kilometers southwards of the School of Health Technology Chafe, the metasedimentary ridge containing the BIF makes a contact with the granite at Chafe.

3.5.1 Megascopic Description

The BIF is dark reddish brown, banded rock with alternation of light grey rich silica and darker iron-oxide rich bands. It is the homogeneous variety and occurs as boulders of different sizes (Plate IX). Texturally, the BIF is fine-grained.



Plate IX: Reddish brown BIF with various boulders displaying the banding (B)

3.5.2 Microscopic Description

The BIF sample was examined under both reflected and transmitted light. The block section examined under reflected light shows that it is granular. It shows distinctive alternation of magnetite crystals and manganese. The magnetite crystal is bright with a granoblastic texture. It is about 50% (visual estimation) of the rock. The green crystal is the manganese minerals; it constitutes about 35% on (visual estimation) of the rock (Plate X). The crystal in form of quartz crystals are yellow, showing wavy extinction when the stage is rotated and fine grain. Quartz constitutes about 10% of the rock (Plate X and XI).

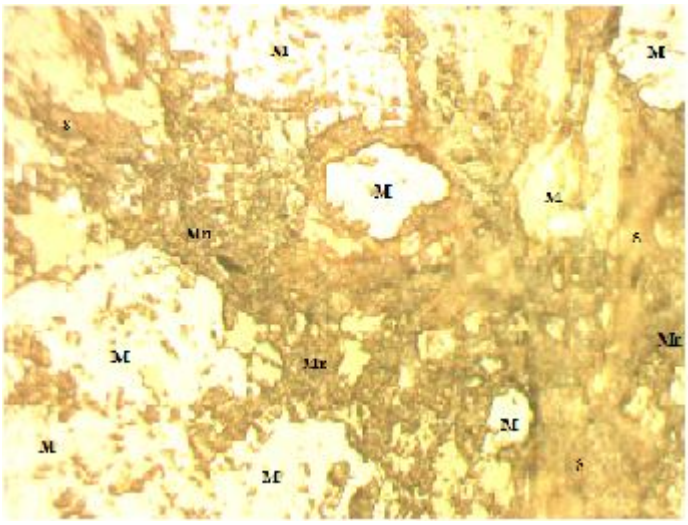


Plate X: Photomicrograph of the BIF block from the study area under the reflected light, M-Magnetite, Mn-Manganese, S-Silicates (quartz) Mg x30.

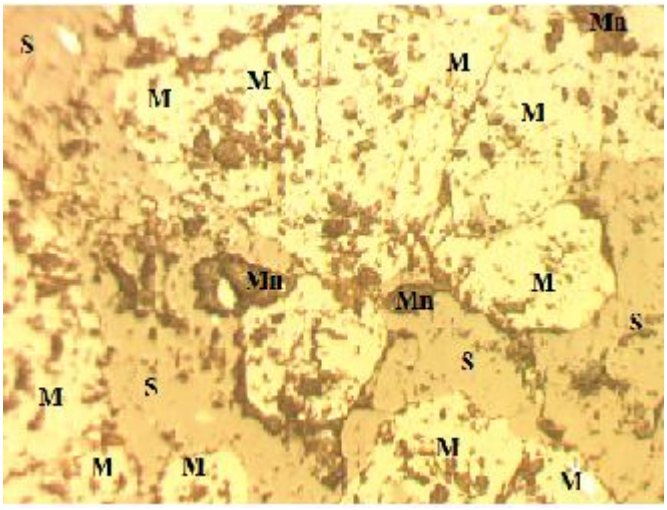


Plate XI: Photomicrograph of the BIF slide under reflected light from the study area M- Magnetite, Mn- Manganese, Silicates (quartz). MG x30

3.6 HORNFELS

The hornfels occurs in Tudun- Wada at the central parts of the mapped area. It occurs as a low-lying dome shaped outcrop (Plate XII). It is light grey to pink in colour and about 500m long and 500m wide with N-S orientation. There are numerous joints and quartz veins observed on the outcrop (Plate 2.3). The rock is fine- grained in texture.



Plate XII: Dome shape of the hornfels outcrop at Tudun-Wada area, N 12^0 01 44' 00", E 006^0 53'00"



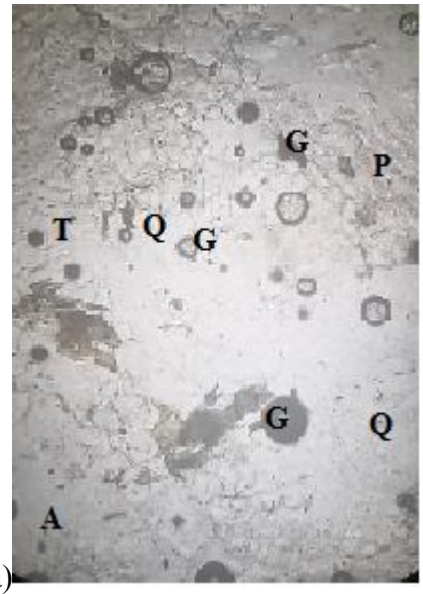
Plate XIII: Quartz 00"vein trending 068^o within the hornfels in Tudun-wada, N 12^0 02 40', 'E 006^0 52' 00"

3.6.1 Megascopic Description

The horfels is light grey, massive with very little or no feldspars seen. The dark coloured mica minerals are more than the quartz and feldspars. Tourmaline crystals are present, black in colour.

3.6.2 Microscopic Description

Sample examined under reflected light shows non-foliated and elongate crystals. It is equigranular in texture. The hornblende as the actinolite forms a needle- like structure with a perfect two directional cleavage and dark brown. It shows pleochroism from brownish to greenish when the stage is rotated (Plate XIV). It constitutes about 70% (visual estimation) of the rock. Plagioclase feldspars are subhedral with light brown colour. It is about 15% (visual estimation). Quartz crystals are colourless in colour with wavy extinction, and constitute about 5% of the crystals that make up the rock. Rounded garnet crystals are about 5%. Tourmaline as acicular or needle-like crystals are present, brown and elongated. It is pleochroic from brown to dark brown with indistinct cleavage. It is about 5% (visual estimation).

(a) 

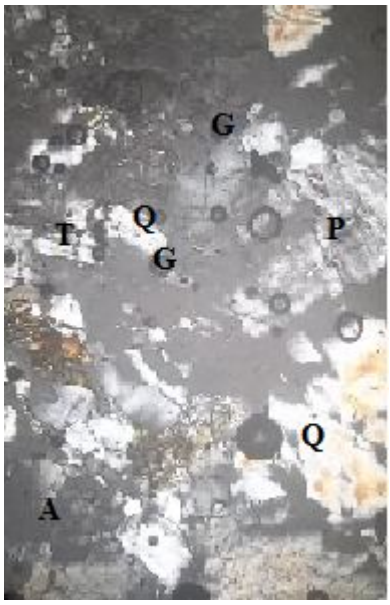
(b) 

Plate XIV: Photomicrograph of hornfels under (a) PPL and (b) XPL displaying randomly oriented crystals. H-Hornblende (actinolite), P-Plagioclse feldspar,Q- Quartz, G-Garnet, T-Tourmaline. MG X10**.**

3.7 GREENSTONE

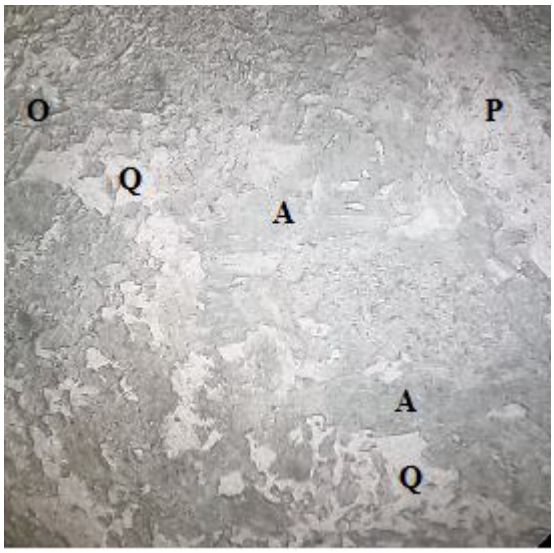
The greenstone is located at Biya-Buki, N 12^{o} 02' 059" and E 006^{o} 50.4'. The rock occurs as low lying outcrop, dark green in colour. It is devoid of structures such as quartz veins, joints and xenoliths. The rock body trends in the general N-S directional trends. It has the N-S orientation.

3.7.1 Megascopic Description

The rock is massive and dark green in colour. It is composed of dark green glassy crystals and little white subhedral quartz crystal with a general fine grained texture. The rock has sharp edges and is heavy in hand specimen.

3.7.2 Microscopic Description

In plane polarized light, the rock is non-foliated and course grained in texture. The Plagioclase feldspars are subhedral exhibiting the albite twinning. It constitutes about 40% of the rock. Quartz crystals are yellowish in colour and granular. It is about 30% of the rock. The light greenish crystals of actinolite crystals are obvious in the PPL, with some opaque minerals. It constitutes about 20% of the green stone rock (Plate XV).

(a) 

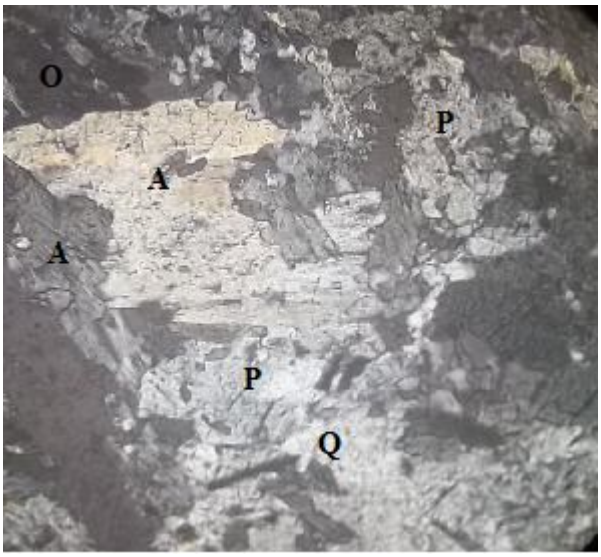
(b) 

Plate XV: Photomicrograph of the greenstone (a) under PPL and (b) XPL A- Actinolite, Q-Quartz, P- Plagioclase feldspar, O-Opaque crystals. MG X10.

3.8 GRANODIORITE

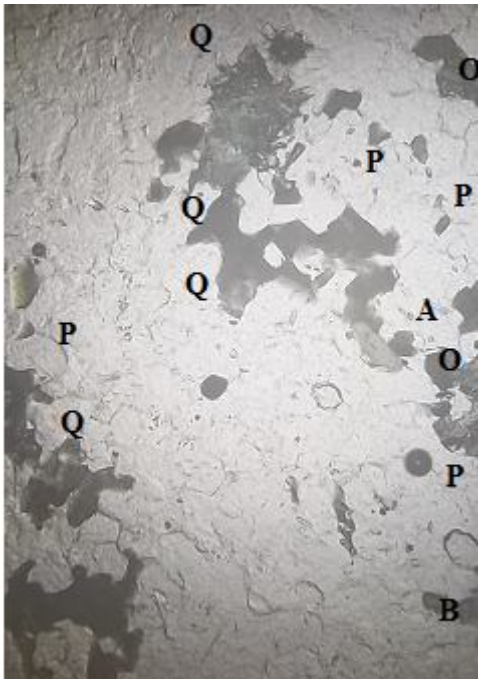
The granodiorite occurs at the northeastern part of the study area around Koha and Butsa villages.. It occurs as low lying outcrops and boulders, with NE-SW trend. The rock makes a boundary with the granitic gneiss at the southwest and diorite to the south and medium grained granite to the north east (Fig.2).

3.8.1 Megascopic Description

The granodiorite in hand specimen is grey in colour with light coloured minerals as the most abundant minerals. The minerals observed on hand specimen are Plagioclase feldspars, quartz and small amount mica minerals. The rock has a fine-grained texture.

3.8.2 Microscopic Description

The rock is non-foliated and fine grained when viewed in transmitted light. Plagioclase feldspar is the most abundant mineral present. It constitutes about 65% of the rock (visual estimation). Quartz crystals are colourless and up to about 25% of the rock. Biotite crystals and opaque crystals constitutes about 10% of the rock (Plate XVI).

(a) 

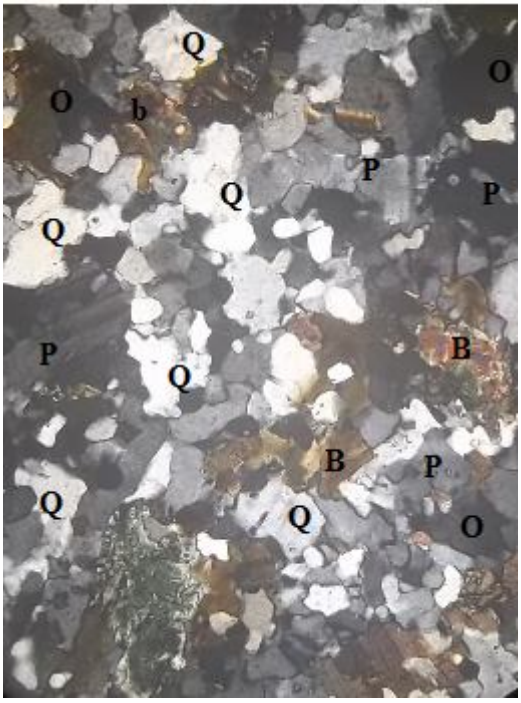
(b) 

Plate XVI: Photomicrograph of Granodiorite under (a) PPL and (b) XPL. P-Plagioclase feldspar, Q-Quartz, B-Biotite, O-Opaque. Mg x10.

3.9 DIORITE

Diorite occurs in eastern part of the study area, north of Mada town. The diorite grades into the granodiorite to the east and north and has an inferred boundary with gneiss to the south (Fig. 2). There is marked gradational transition from diorite-granodiorite-granite along traverse lines to the northeast.

3.9. 1 Megascopic description

The diorite observed in hand specimen exhibits course grained texture and is composed of mainly mafic minerals, though plagioclase feldspars are present. Megacryst of mafic crystals is about 3 centimeters are observed surrounded by the ground masses of quartz and feldspars. The crystallization of the diorite seems to be post-tectonic due to the absence of joints trends on the outcrop. Minerals observed in hand specimen are micas, plagioclase feldspars and quartz. Due to the severe weathering of the rock no thin section was made.

3.10 MEDIUM GRAINED BIOTITE GRANITE

The medium grained biotite granite occurs mostly in the extreme south eastern part of the study area, from extreme southern boundary of the study area around Magazu town north of Chafe town and occurs as whale back exposures (Plate XVII), the granite dips 045^{o}.



Plate XVII: Medium grained biotite granite ridge at Chafe.

The granite is light grayish in colour with N-S general orientation. Boulders of medium- grained biotite granite were observed at the bottom or foot of the granitic rock (Plate XVII). The medium- grained granite is elevated to an average altitude of about 1850 metres (Fig.2) and cut across the major road leading to Gusau town from Funtua. The rock is grey generally. The granite extends up to the end of the southern boundary at Magazu town. The rock is well jointed mostly in N-S direction. The texture of the granite varies from medium, course to porphyritic.



Plate XVIII: Boulders at the foot of the granitic ridge located at Chafe 11^0 55 22' N, 006^0 56 18'E



Plate XIX: Joints on the granitic rock at Chafe, 11^0 56 18' N, 006^0 55 12'E

3.10.1 Megascopic Description

The granite observed in hand specimen is light grey in colour with medium grained texture. Minerals present are feldspars, quartz and micas.

3.10.2 Microscopic description

The rock MA14 examined under the microscope is mainly characterised by quartz rich and the biotite crystals. The rock is generally medium-grained in nature with quartz as the most abundant crystals present, about 35% (visual estimation). The quartz is anhedral and colourless with the characteristic wavy extinction. Biotite crystals are brown with its distinct one directional cleavage. The biotite constitutes about 30% of the rock. Microcline exhibiting the Carlsbad twinning makes up about 20% of the rock. Plagioclase feldspar is present about 5% (visual estimation) (Plate XX).

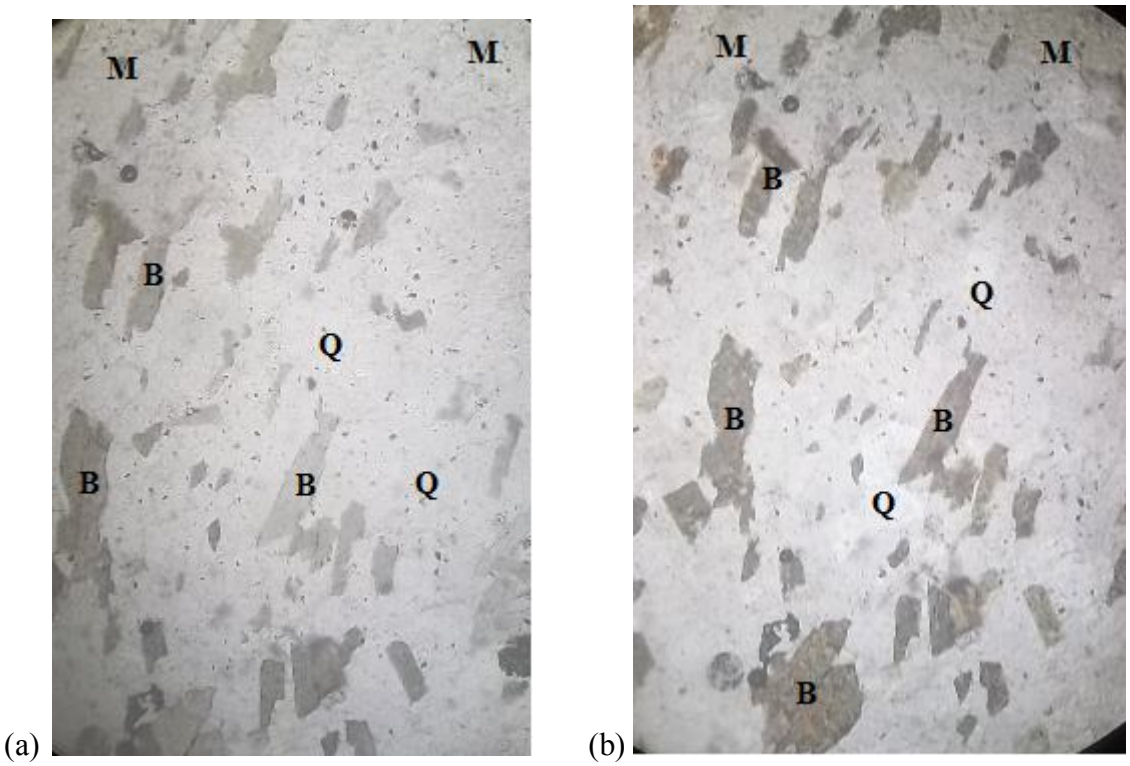


Plate XX: Photomicrograph of medium grained biotite granite from Chafe (a) under PPL and (b) XPL Q- Quartz, B-Biotite, Q- Quartz M-Microcline feldspar Mg x10

3.11 PORPHYRITIC GRANITE

The porphyriric granite occurs as an intrusion within the granitic rock at Chafe. The porphritic granite intruded the medium-grained granite. It has a general northsouth orientation.



Plate XXI: Porphyritic texture at some part of the granite at Chafe.

3.11.1 Megascopic Description

The rock MA15 of the porphyritic granite in hand- specimen is light grey. The minerals observed in the rock are pink feldspars, quartz and biotite. The rock has a porphyritic texture.

3.11.2 Microscopic Description

The rock MA15 examined under PPL shows granular texture. Plagioclase feldspars are subhedral exhibiting the albite twinning and constitute about 40% of the rock. Quartz crstals are colourless crystals present are subhedral. It is about 20% of the total rock composition. The light green anhedral crystals are the hornblende, occurs as plates and small elongate needle like crystal grain with fine matrix and shows preferred orientation. It constitutes about 20% of the rock. Biotite crystals are present, it is about 15% of the rock, brown in colour in an oriented structure (Plate XXII). Dark opaque minerals constitute about 5%.

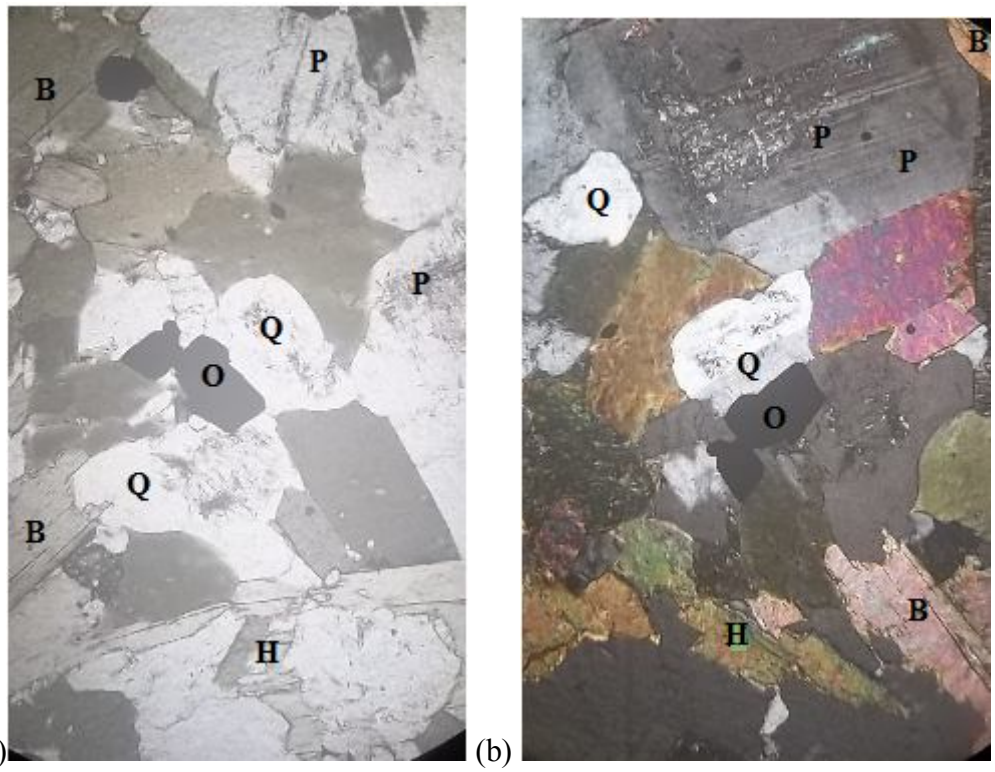


Plate XXII: Photomicrograph of the Porphyritic granite under (a) PPL and (b) XPL P -Plagioclase feldspar, Q-Quartz, H-Hornblende B-Biotite, O-Opaque minerals. Mg x10.

3.12 STRUCTURES

Rocks in the study area are generally well exposed in some areas so that simple structural features such as joints and faults are conspicuously observed. The joints and faults are formed probably as a result of brittle deformation while foliation and folds observed on the outcrops are formed as a result of ductile deformation of rocks in the study area.

3.12.1 Joints

Joints in various directions are present in nearly all the exposed rocks in the study area. The joints are more pronounced in the granitic rocks (Plate XXIII). Two sets of joints were observed in the study area and are grouped into minor and major joints with N-S and NNE-SSW trends respectively. They are steeply dipping and parallel to the foliation planes. Some of the joints have been filled with quartz while others are barren. Joints measurements were undertaken (Appendix C) and all the measured joints planes in the area of study were plotted on rose diagram (Fig. 6). This has led to the recognition of NNE-SSE joint set which is well defined.

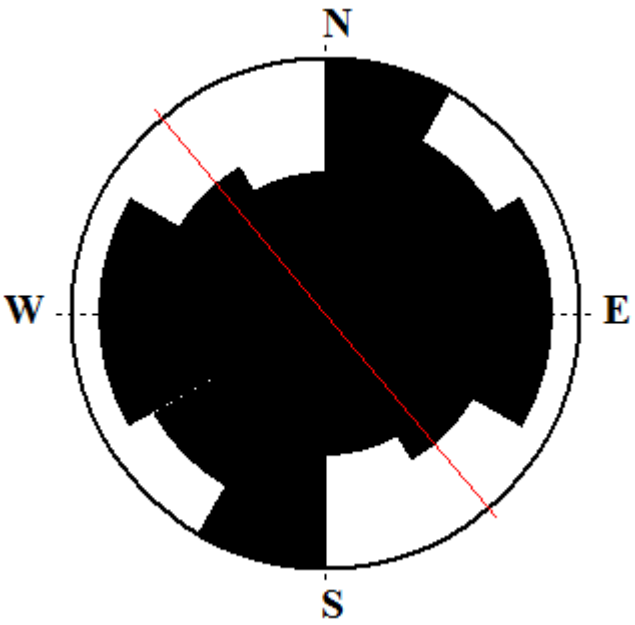


Figure 3.2: Rose diagram for the joints measured in the study area.

The NNE-SSW trend in the above rose diagram may represents the Pan-African orogeny, while the E-W represents the older tectonic events possibly the Eburnian orogenic cycle.



Plate XXIII: Photograph of cross cutting joint trend in granitic-gneiss.

3.12.2 Foliations

Most of the rocks in the study area are foliated. This is well displayed in the gneisses and schist rocks. Foliation in the gneisses is defined by the parallel alignment (banding) of felsic and mafic minerals in the NE-SW directions. In metasediments and schistose rocks such as in phyllite, the foliation directions are defined by the parallel orientation of platy minerals (Plate XXIV). In the granites, the foliation is weak and is marked by the aligned biotite that impacts a weak foliation on the rock.



Plate XXIV: Photograph of Phyllite exhibiting NE-SW foliation trend at 12^0 05 4'N, 006^0 52' in the study area.

3.12.3 Faults

A dextral fault was observed on a diorite exposure around Mada, in the northern part of the study area. A dextral type displacement of 50 centimeter apart was observed of an aplite dyke in the diorite (Plate XXV).



Plate XXV: Photograph of a faulted aplite dyke in a diorite in the study area north of Mada, 12^0 09'N 006^0 56'

3.12.4 Fold

A simple asymmetrical fold was observed on the silicified muscovite schist interbedded with thin layers of carbonaceous schist in the study area (Plate XXVI). The schist strikes N17^{o} E and dips 053^{o}.

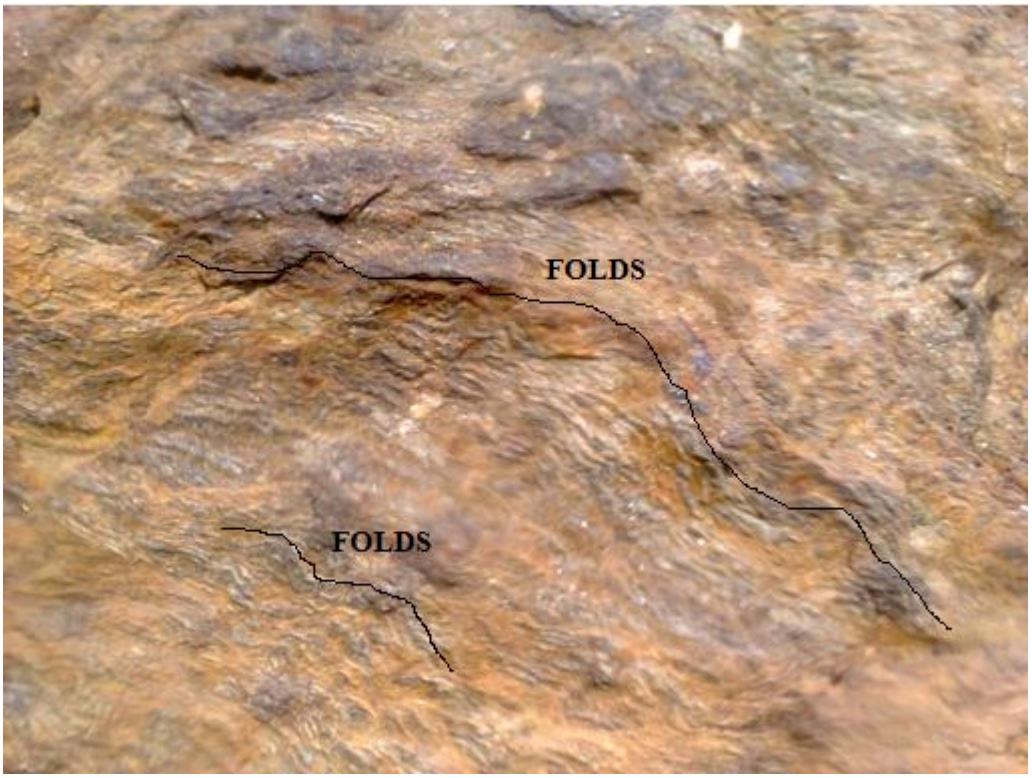


Plate XXVI: Photograph of a simple asymmetrical fold on the muscovite schist at 12^{0} 05'N 006^{0}52'E

CHAPTER 4

GEOCHEMISTRY

4.1 SAMPLING AND ANALYTICAL TECHNIQUES

Representative samples of the various rock types collected from the study area along selected traverse lines were selected for analysis. These include two granite-gneisses, one gneiss, two biotite muscovite schist, four BIF's, one hornfels, one greenstone rock, two granodioritic rock and two granitic rocks. Determination of major and trace elements were carried out using X-Ray Fluorescence technique at Kano University of Science and Technology. In addition to XRF technique, Flame Photometry analyses for the same rock samples were carried out at the Centre for Energy Research and Training (CERT), Ahmadu Bello University Zaria.

4.2 RESULTS

The results generated are presented in Tables 2,3,4,5 and 6. The data generated is used for the calculations of the average major, trace and lithophile element composition. The data was interpreted using a geochemical data tool kit (GCD Toolkit 3.0).

Table 2: Major elements compositions of rocks from the study area (values in wt %)

Samples/ oxides	MA1 Granitic gneiss	MA2 Granitic gneiss	MA3 Gneiss	MA4 Biotite Muscovite schist	MA5 Biotite Muscovite schist	MA6 BIF	MA7 BIF	MA8 BIF	MA9 BIF	MA10 Hornfels	MA11 Green stone	MA12 Granodiorite	MA13 Granodiorite	MA14 Medium grained biotite granite	MA15 Porphyritic granite
SiO_2	80.03	73.12	79.32	61.42	63.73	50.75	50.59	51.21	50.29	51.03	74.24	75.05	73.04	72.86	67.01
Al_2O_3	12.03	12.37	12.31	14.89	14.38	5.29	6.11	5.71	5.38	14.05	13.46	16.70	15.67	11.98	12.00
Fe_2O_3T	0.81	1.38	1.44	9.52	7.68	41.62	40.79	40.50	39.76	8.41	3.94	2.12	2.27	2.48	6.29
CaO	0.91	0.79	1.52	0.96	0.81	0.48	0.52	0.42	0.57	15.67	2.83	0.02	0.03	2.04	1.11
Na_2O	0.10	0.12	0.06	0.42	0.39	0.02	0.02	0.03	0.03	0.28	0.22	0.07	0.06	0.10	0.20
K_2O	4.45	4.35	6.04	9.36	7.26	0.03	0.03	0.04	0.04	0.08	6.34	2.97	2.82	5.08	5.84
TiO_2	0.73	0.63	1.29	1.25	1.24	0.87	0.76	0.83	0.69	0.33	0.51	0.20	0.22	0.43	0.22
MnO	0.02	0.03	0.08	0.54	0.43	4.37	4.53	3.89	5.39	0.14	0.06	0.05	0.06	0.04	0.16
TOTAL	99.05	92.79	103.06	98.36	95.92	103.43	103.66	103.28	103.28	89.99	101.60	97.18	94.17	94.38	92.86

Table 3: Calculated total elemental iron and manganese of the BIF's

SAMPLE	% Fe	% Mn
MA6	29.11	3.38
MA7	28.53	3.51
MA8	28.33	3.01
MA9	27.81	4.17

Table 4: Trace elements compositions of rocks from the study area (ppm).

Samples/ elements	MA1 Granitic gneiss	MA2 Granitic gneiss	MA3 Gneiss	MA4 Biotite Muscovite schist	MA5 Biotite Muscovite schist	MA6 BIF	MA7 BIF	MA8 BIF	MA9 BIF	MA10 Hornfels	MA11 Green stone	MA12 Granodiorite	MA13 Granodiorite	MA14 Medium grained biotite granite	MA15 Porphyritic granite
K	36983	38761	50177	77715	53636	155	141	175	114	683	52657	24623	1414	42137	48520
Ba	254	312	1487	983	822	1048	997	1072	1297	324	1056	953	514	701	566
Rb	253	219	123	575	219	9.3	8.4	6.3	LOD	2.4	229	84	190.8	184	536
Sr	282	187	06	243	87	29.5	28	19	27	212	1102	1414	82	401	114
Zr	138	442	566	524	480	327	350	255	149	63	666	257	29	440	293
Pb	46	71	68	49	27	LOD	LOD	LOD	LOD	LOD	55	52	LOD	39	42
W	346.5	310	320.4	135.4	160	312.3	289	LOD	337.6	180.1	188.8	191.5	201	246.5	128.5
Zn	83	77	168	195	60	210	167	204	236	94	109	80	167	95	156
Ni	58	154	78	112	58	407	421	598	398	80	92	69	1078	70	101
Cr	12	17	38	149	96	156	148	110	148	79	95	43	LOD	24	95
Co	136	240	244	1369	761	LOD	LOD	LOD	LOD	1207	669	358	LOD	342	644
V	306.8	LOD	1069	646.9	380	152.2	139	LOD	LOD	300.1	525.8	645.1	LOD	436.6	354.6
Bi	41.3	78	42	51.2	38	36.4	29	28	33	LOD	52.5	16.5	LOD	77.5	49.1
Se	16.3	18.8	15.5	5.9	10.8	11	09	17	LOD	14.4	11.3	6.8	13	12	4.5
Cu	LOD	58	86	172	104	349	312	191	195	134	139	84	224	86	41
Hg	103	87	92	52	35	80	68	111	LOD	55	52	36	68	64	29
Hf	44.6	49	LOD	LOD	56	LOD	LOD	LOD	LOD	57.9	LOD	40.7	LOD	LOD	LOD
Ag	29	58	50	80	46	174	LOD	LOD	LOD	81	63	36	LOD	46	54
As	LOD	LOD	LOD	LOD	LOD	LOD	28	24	LOD	LOD	11	LOD	82	LOD	LOD

LOD= Limit of detection

Table 5: Lithophile elements composition (PPM)

Samples /element	MA1 Granitic gneiss	MA2 Granitic gneiss	MA3 Gneiss	MA4 Biotite Muscovite schist	MA5 Biotite Muscovite schist	MA6 BIF	MA7 BIF	MA8 BIF	MA9 BIF	MA10 Hornfels	MA11 Green stone	MA12 Granodiorite	MA13 Granodiorite	MA14 Medium grained biotite granite	MA15 Porphyritic granite
K	36983	35897	50177	77715	72631	155	141	158	160	683	52657	24623	25532	42137	48520
Ba	254	312	1487	983	822	1048	987	1072	1297	324	1056	953	719	701	566
Rb	253	219	123	575	219	9.3	LOD	6.3	LOD	2.4	229	84	68.3	184	536
Sr	282	187	1506	243	87	29.5	25.5	29	31.2	212	1102	1414	1300	401	114

Table 6: Lithophile elements ratio

Samples/element	MA1 Granitic gneiss	MA2 Granitic gneiss	MA3 Gneiss	MA4 Biotite Muscovite schist	MA5 Biotite Muscovite schist	MA6 BIF	MA7 BIF	MA8 BIF	MA9 BIF	MA10 Hornfels	MA11 Green stone	MA12 Granodiorite	MA13 Granodiorite	MA14 Medium grained biotite granite	MA15 Porphyritic granite
K/Ba	146	115	79	79	88	0.15	0.14	0.15	0.12	2	49	25	36	60	86
K/Rb	146	164	407	135	332	17	LOD	25	LOD	285	229	293	373	229	91
Rb/Ba	0.99	0.70	0.08	0.58	0.26	0.01	LOD	0.01	LOD	0.01	0.21	0.01	0.01	0.26	0.95
Rb/Sr	0.89	1.17	0.08	2.36	2.51	0.31	LOD	0.21	LOD	0.01	0.20	0.05	0.05	0.45	4.70

4.3 DISCUSSION

4.3.1 Major Element Composition

The major rock types underlying the study area comprise of, granitic gneiss, gneiss, biotite-muscovite schist, BIF, hornfels, greenstone, granodiorite, and granitic rocks. The major elements analysis shows that the rocks are characterized by high SiO_2 in the range of 50.29 - 84.03wt % with an average of 60.77wt%. Low content of Fe_2O_3 (0.81- 6.29 wt %) with the lowest content in the granitic gneiss, moderate content (7.68 -9.52 wt %) and the highest content in the BIF (41.62 wt %). In addition, soda remains consistently less than potash in almost all the rock types except for hornfels (MA10), Table 2.

Alumina (Al_2O_3) contents for all the rock types are generally within the range of (5.29-16.70 wt %). This values falls within the average continental contents of these rocks. Also, the rocks have aluminum saturation index [defined as the molar ratio of Al_2O_3/ ($CaO+Na_2O+K_2O$) after Ekwume (2003)] greater than one (1) and consequently falls within the corundum norm except for the hornfels (MA 10) with Al_2O_3/ ($CaO+Na_2O+K_2O$) < 1 probably due to high content of CaO even greater than Al_2O_3, hence cannot have corundum in it norm.

TiO_2 and SiO_2 composition of the rock samples in the study area were plotted in TiO_2-SiO_2 discrimination diagram (Tarney, 1977); in an attempt to determine the nature of their protolith (Fig 4.1).

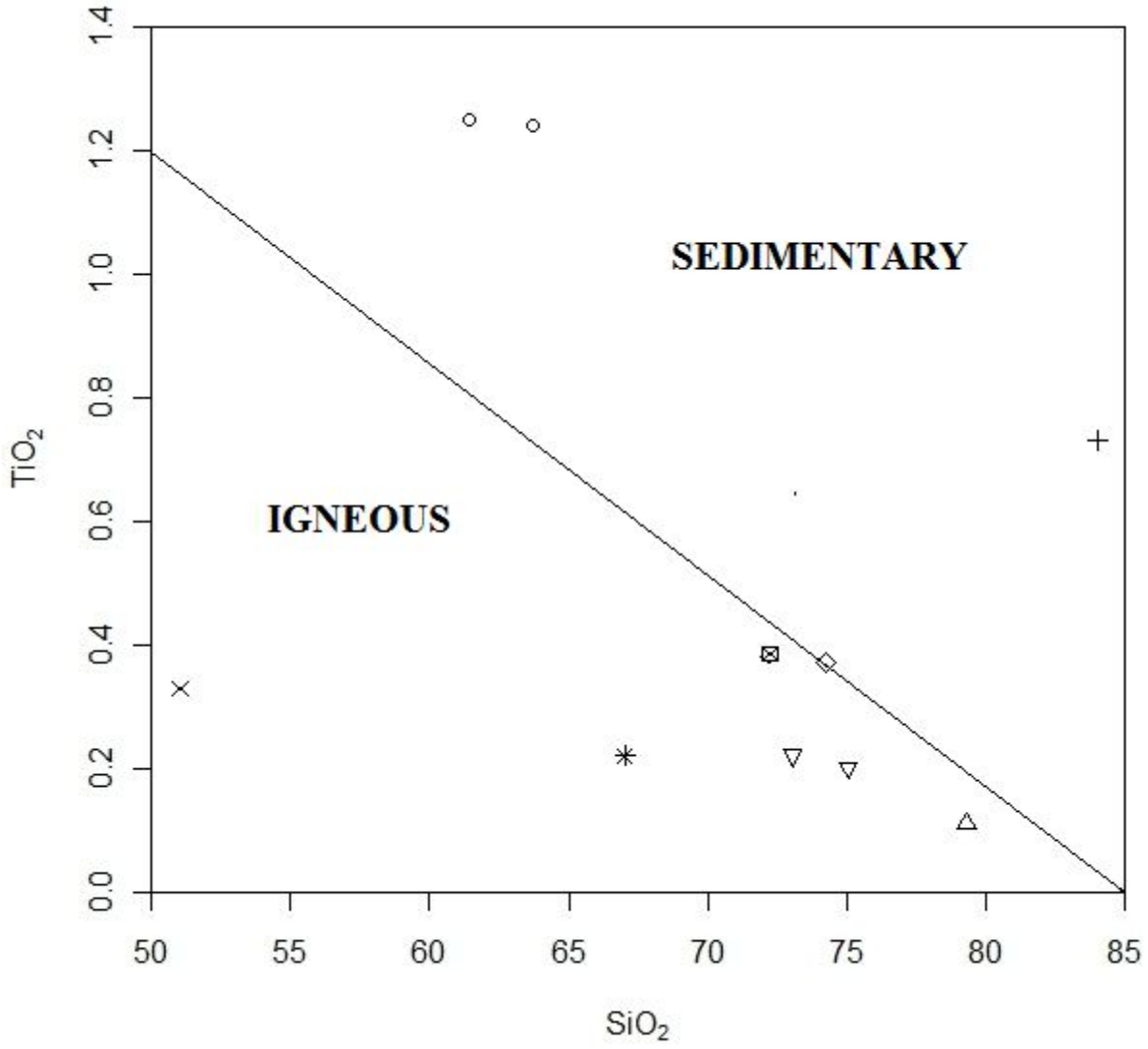


Figure 4.1: TiO_2 versus SiO_2 discrimination diagram (after Tarney, 1977). Showing the nature of the protholith of the granitic gneiss, gneiss, biotite muscovite schist, hornfels, greenstone, granodiorite, medium grained biotite granite and porphyritic granite. Line separates sedimentary from igneous protholith.

Figure 4.1 reveals that granitic gneiss, biotite muscovite schist and greenstone have sedimentary protholiths, while gneiss, hornfels, granodiorite, medium grained biotite granite and porphyritic granite (MA 15), are from igneous protholith.

SiO_2+Al_2O_3 concentration as well as total elemental concentrations of (Fe+Mn) in the BIF samples MA6 (56.04 wt% and 34.49wt%,), MA7 (56.70wt% and 32.49wt%,), MA8 (56.92wt% and 31.34wt%), MA9 (55.67wt% and 33.98%). These values are comparable to the values obtained from Unguwar-Malam Ayuba iron- formations in north western Nigeria that reveal a wide range of composition with respect to their (SiO_2+Al_2O_3) and Fe+Mn concentrations which range from 70-40 and 40 to 18 wt% respectively (Mucke et al.,1994).

Comparison of the chemical composition of the BIFs in the study area with associated rocks and other Nigerian iron-formations with similar settings clearly reveals some similarities. For example, Tables 2 and 4 above show that BIFs have relatively high Mn (3.89 — 5.39wt%), Fe(39.67—41.62wt%) and low alkalis [Na(0.02— 0.03wt%), K(0.03 — 0.04wt%) and Rb (2.4—9.3ppm)], Sr (29.5 — 97ppm), Ti (0.69—0.87ppm), Al (5.29 — 6.71wt%) and Si (50.29 — 51.21 wt%) but the associated rocks show opposite in character such as low Mn (0.02-0.08wt%), Fe (0.81-9.52 wt%) and high alkalis [Na(average of 0.06 —0.42 wt%), K (0.08 — 9.36 wt%), Rb (2.4 — 575 ppm)], Sr (06 — 1414 ppm), Ti (0.22-1.24wt%), Al (11.98 — 16.70 wt%), Si (61.42 —84.03 wt%). These values are comparable to the values of other northern Nigeria iron-formations such as that of Birnin-Gwari with high Mn (5.98 wt %), Fe (42.84 wt%), Al (7.93 wt%), Si (50.59 wt%), alkalis [Na(0.02wt%), K (0.04 wt%) except for Rb and Sr that shows a slight variations of (1.1ppm and 48ppm) respectively (Mucke et al., 1996). The above dissimilarities in chemical compositions between the BIF and the associated rocks clearly suggest a difference in origin between the BIF and the associated rocks.

The high amount of Fe and Mn in the BIF [Mn (5.39wt%), Fe (41.62wt%)] may be as a result of supergene enrichment in the iron-formation, as envisaged by Adekoya, (1996), who showed that the Mn is enriched in the oxide facies iron formation of Nigeria from 1.4% to 4.5% and the Fe enriched from 25% to 35%. This is as a result of repeated leaching and redeposition of Fe and Mn oxide within the enrichment zone.

In addition, when MnO and FeO(tot) composition of the BIFs (MA 6, MA7, MA8 and MA9) in the study area was plotted in MnO-FeOtot discrimination diagram (Mücke 2005);

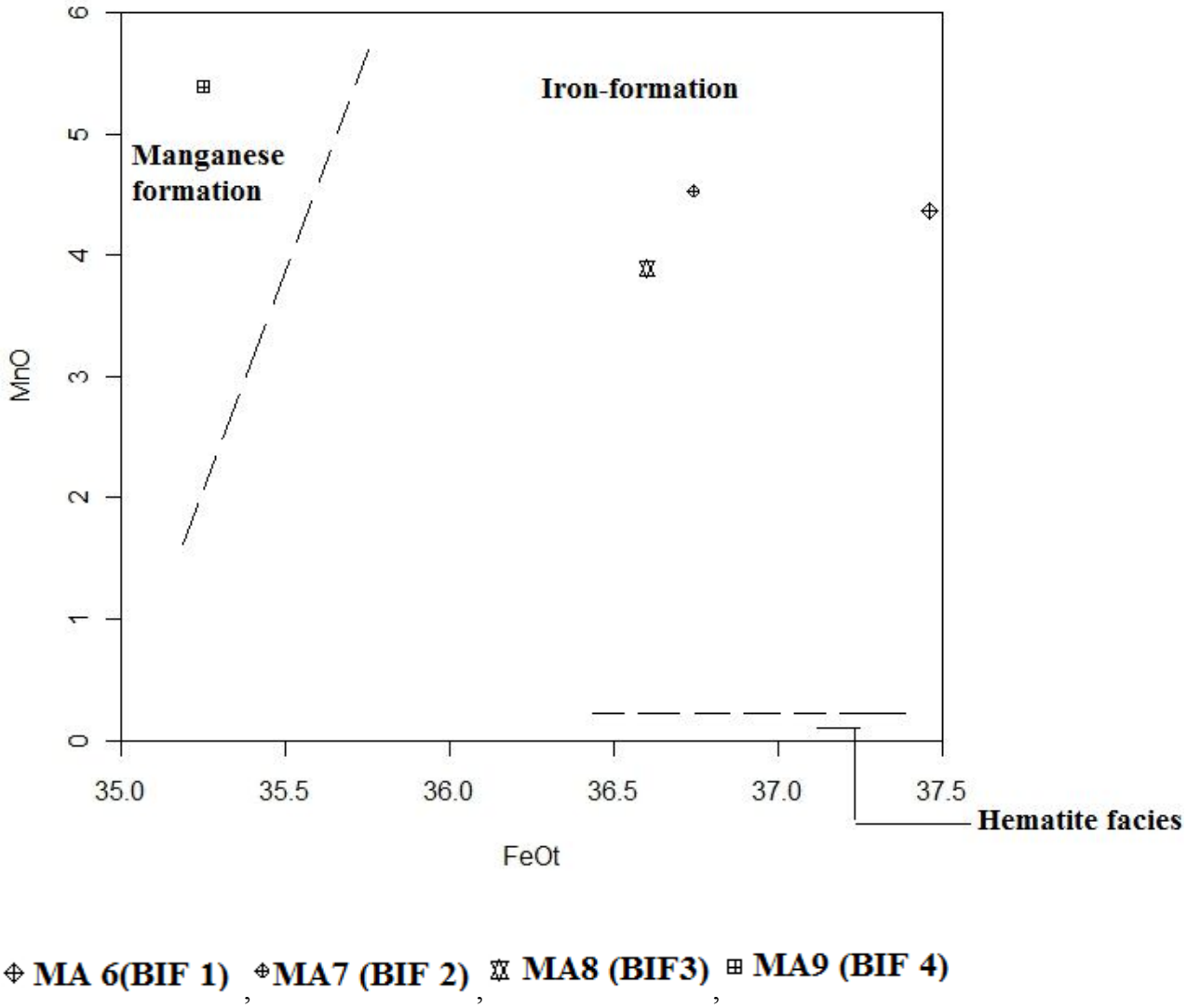


Figure 4.2: MnO/FeO(tot)- diagram (wt %), (Mücke, 2005) BIF sample in the study area showing the manganese formation and iron-formation areas.

Figure 4.2 shows that the BIF in the study area contain high Manganese and iron concentrations. This is in agreement with Mucke (2005) that contrary to many other iron-formations, those of Nigeria are characterized by their high manganese concentrations.

4.3.2 Trace elements composition

Chemical data for the trace elements is presented in Table 4. Cr, Ni and Zn in the BIF sample show a significant increase in their concentrations as compared with their concentration in the associated rocks. However, the BIF is depleted in Co and V. The sources of these ferromagnesian elements are generally mafic rocks. The enrichment of these elements in the BIF could help in tracing the possible precursor to the BIF (Ibrahim, 2002). The elements Co, Ni Cu and Zn are used to find the possible precursor to the BIF in the area (Bonatti et al., 1972). The high concentrations of Cr, Ni elements suggest that the precursors of the BIF may include a terriginous ultramafic to mafic suites.

4.3.3 Lithophile Element Distribution Pattern

Lithophile elements (K, Rb, Ba, Sr) abundances and their relationship presented in Tables 5 and 6 show some meaningful pattern.

Generally, there is marked enrichment of most of the lithophile elements of all the rock types in the study area except for the BIF that shows a kind of depletion of the lithophile elements. Like K (683-77715 ppm), Ba (254-1487 ppm) Rb (68.3-575ppm) except for the hornfels (2.4 ppm), Sr (114-1506ppm) in all the rock types except for the BIF, K (141-160 ppm), Rb (6.3- 9.3 ppm), Sr (29.5-97ppm). But Ba (987-1297 ppm) shows marked enrichment in the BIF compared to the associated rocks.

The Sr concentration of the BIFs in the study area is averagely 28.8ppm. This value is comparable with values of other BIF deposit, for example the value obtained for Koriga 24ppm (Okwonkwo,1991).

The K/Rb ratios in Table 6 for hornfels, greenstone, granodiorite and medium grained granite are within the range of 226-415 ppm. These values are similar to the values obtained by Tailor (1969) indicating Rb depletion. K/Rb ratios are considered to be within the range of 150-300. The abnormally high K/Rb ratios exhibited by granodiorite could be due to the accumulation of early feldspars which are depleted in rubidium.

4.3.4 Origin of the Iron-formations (The BIF)

The BIF in this study is located in a metasedimentary terrain of Wonaka schist belt that is composed of metasedimentary and metavolcanic rocks. The BIF in the study area is similar to that of Maru and Birnin-Gwari in terms of texture; both are fine-grained with similar mineralogical compositions of magnetite, quartz and other accessory minerals. The Al_2O_3- concentration (5.62 wt % on average) of the BIF in the study area is comparable to the range of values of Al_2O_3-concentration of other BIF values at Unguwar- Malam Ayuba (ranging from 2.3 to 18.5 wt %) as revealed by Mucke (1994).

The high Al-content in the Nigerian iron-formations is probably as a result of the continuous supply of continental material into the marine basin. Therefore, it can be deduced that the SiO_2-content of the iron-formation is not necessarily from the exhalative origin only but may also be of continental origin.

This BIF therefore could be taken to belong to the silicate facies type that has been exhaustively studied by several workers such as Ibrahim, (2002); Adekoya, (1996); and Mucke et al. (1996) in

many NW, central and SW Nigeria occurrences. Terrigeneous source is envisaged to have provided the material for the BIF. This is based on trace element composition Zr, Rb and Sr; these elements are part of the few elements brought to the ocean water by weathering of felsic rocks of the crust (Ibrahim, 2002). The enrichment of these elements may be considered as indications for the supply of the BIF sequence. These elements have all shown a considerable degree of enrichment in this BIF (Table 4).

Similarly, Ibrahim (2002) agreed that Ni, Cr, Co and V are ferromagnesian elements that are sourced from mafic rocks in accordance with Khan et al.(1996). Therefore enrichment in the abundances of Ni, Cr, Co and V as exhibited by this BIF indicates basic-ultrabasic material was one of the major contributor to the basin of deposition.

It is now widely believed that the materials for the formation of BIF globally are derived from two main sources: continental granitic rocks and volcano-sedimentary deposits (Khan et al.,1996,; Adekoya, 1996; Mucke et al.,1996; and Ibrahim, 2002),. A ternary plot of Fe-Mn-(Co+Ni+Cu+Zn)*10 is plotted for the BIF in the study area. The diagram (Fig. 4.3) shows that the BIF is from submarine-hydrothermal source.

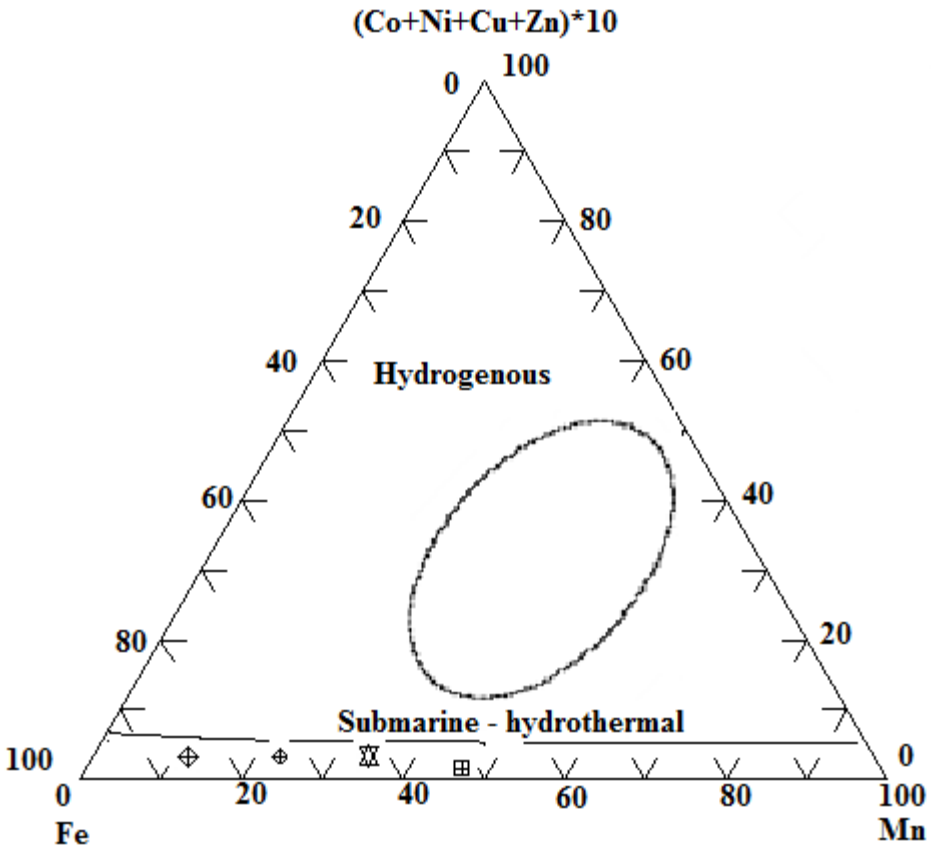
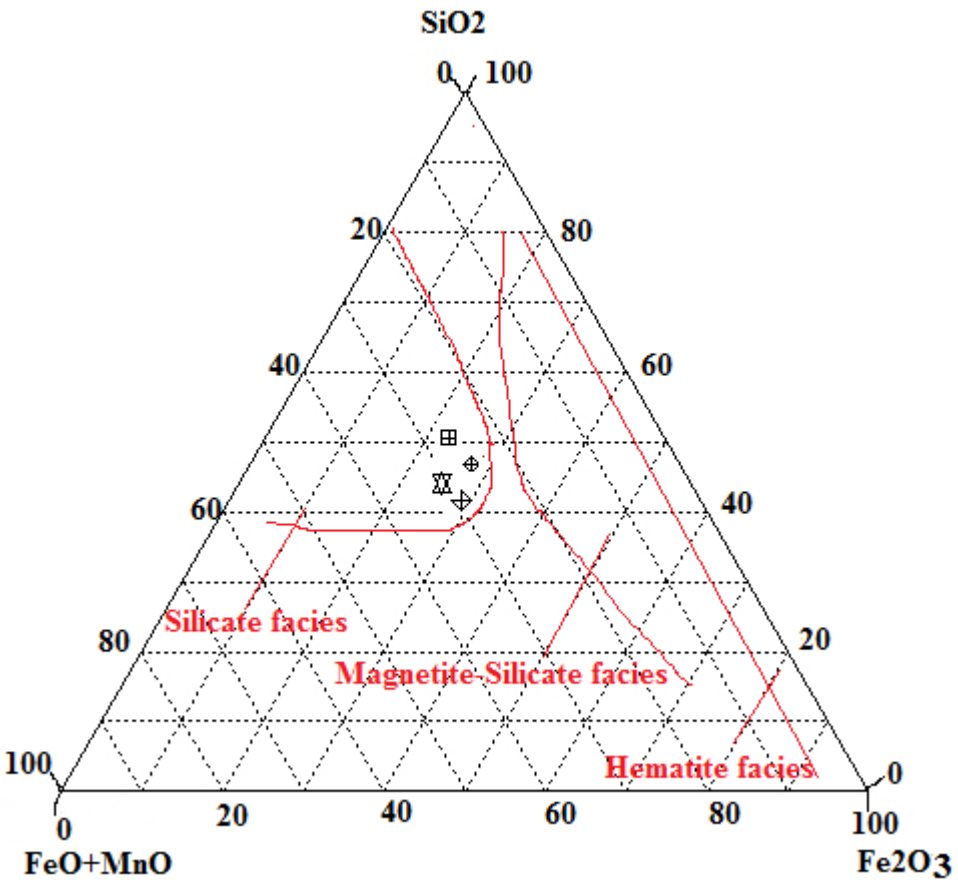


Figure 4.3: Fe-Mn-(Co+Ni+Cu+Zn)*10- diagram to differentiate submarine hydrothermal and hydrogenous deposit (Bonatti et al., 1972) and the analytical plot of the BIF in the study area.

Based on figure 4.4 below, the BIF in the study area falls within the field of silicate facies and lies close to the (FeO+MnO)-SiO_2 join**.**

Therefore, the BIF in the study area is of the silicate facie type. It is the most wide spread type of iron formation in Nigeria that is developed in all the schist belt of northern Nigeria especially in the Malumfashi in (Tudun Kudu and Unguwar Malam Ayuba areas), Birnin-Gwari schist belts and in Isanlu in Central Nigeria (Mucke et al., 1994) and that of Kazaure schist belt(Danbatta, 1999; Ibrahim, 2002).



⌖ MA 6(BIF 1) , ⌖MA7 (BIF 2) , ⧖ MA8 (BIF3) , ⊞ MA9 (BIF 4)

Figure 4.4: A ternary plot of SiO_2; FeO + MnO; Fe_2O_3, (After Mucke, 2005). The BIF's in the study area all fall within the silicate facie type.

CHAPTER 5

MINERALISATION POTENTIAL OF THE STUDY AREA

5.1 PREAMBLE

Having discussed the petrography and geochemistry of the major rock types in the study area, it is now established that most of the major rock types from the study area do not present major mineralization potential for economic minerals, but their associated minerals could be used industrially. However, the granite at Butsa in the northeastern boundary of the study area has potential for alluvial placer gold. The BIF occurance at Bayan- Banki village has potential for iron.

5.2 GOLD

A potential site for gold is located at lat.12^{o} 12$^{'}$54.00$^{"}$ N and long. 07^{o} 00' 26.21"E in Butsa village. The site is located about 12.5 km NE of Mada situated around low-lying medium grained granite. The medium grained granite is highly weathered with NE-SW orientation. Outcrops of this rock occur within River Gajere.

The gold mineralization here is secondary alluvial type (placers). It is observed that the typical locations of the gold placer deposit are inside the bends, creeks and at a break of slope of the river. For the gold to have accumulated in the placers, the gold particles might have resisted the weathering process, denser than the flowing alluvium soil as quartz constitute the larger component of the sand and water velocity remains below the required to transport them further.

The source of the gold could have travelled from a far distant lode for the fact that the gold observed in hand specimen has smooth round surfaces or flakes, which is a function of the distance travelled from its source, otherwise, the gold surfaces would have had rough surface suggesting a nearby source lode. According to the artisanal miners, for each one pan of full alluvium sand washed, about 1 to 1.5 mg of gold is won (Plate XXVII)



Plate XXVII: Photograph showing artisanal mining of gold won using a local sluice machine.

However, artisanal gold mining is the major activities taking place in the area. The small scale gold miners use a local sluice box machine to sieve the gold from alluvial placers (Plate XXVII).



Plate XXVIII: Artisanal miners using a local sluice box machine to sieve the gold from the alluvium soil.



Plate XIX: Artisanal miner using the local pan to wash the gold in River Gajere.



Plate XXX: Artisanal miners carrying their local tools for their artisanal gold mining activities.

However, physical features such as durability, chemically-inert, rare and beautiful qualities of gold makes it useful for monetary exchange and investment, jewelry and art. Gold high electrical conductivity, malleability and ductility make it useful as an industrial metal. Gold is alloyed with silver, copper, nickel, palladium, zinc titanium to increase its tensile strength.

The gold-bearing conglomerates at Zamfara state may represent an ancient alluvial deposit, formed long after the emplacement of the auriferous quartz veins in the schist. It is also possible that the gold was deposited from solutions, which ascended along plane of weakness in the shatter belt (Russ, 1957). It is possible that, during the long period of erosion to which the gold area is subjected, gold have been progressively concentrated in the river systems. That considerable

concentration that has taken place is demonstrated by the much greater gold production from the alluvial deposits than from all other source (eluvial, lodes and conglomerates).

According to Garba (2005), the origin of gold and rare metal pegmatite mineralisations is more controversial because of their spatial association with various rock types. For example, gold mineralization hosted by metamorphic rocks were ascribed to regional metamorphic sources, while those associated with granitoids were thought to have magmatic origin (Woakes and Bafor,1984, Garba, 1988).

Gold-quartz-sulphide (± carbonates) veins occur in many places, mostly associated with the schist belts of the west half of Nigeria. Prominent occurrences are known from Anka-Maru, Bin Yauri and Birnin Gwari areas in the northwest, through Minna area. These areas have epigenetic gold-quartz sulphide (veins) hosted by different rock types.

However, previous studies (Garba, 1992, 1996, 2000, Garba and Akande, 1992) have described the occurrence and shown that ore fluids involved were probably generated along regional fault system and focused into the metasedimentary country rocks before deposition of the gold mineralization at the granodiorite contact. The role of granodiorite as a source of ore fluids have been ruled out.

The possible fluid source in all the gold mineralization sites studied in Nigeria basement may be an indication of gold ore fluids active on regional scale. The structural settings also suggest the emplacement of the gold to be late Pan African, subsequent to peak regional metamorphism and granitoid intrusion. This was also a period (c 500 Ma) characterized by widespread uplift and brittle deformation which give rise to the development of regional fault conjugate system (Anka and the Kalangai faults) which are often associated with locally developed subsidiary (NW-SE)

sinistral fault (Fig. 5) that host the gold mineralization. The spatial relationship between the gold mineralization and transcurrent fault systems that were possible Pan-African crustal sutures (Wright, 1976; McCurry and Wright, 1977; Ajibade and Wright, 1989) suggest a genetic link with collision tectonics. This appears to be applicable to mesothermal (orogenic) gold deposit all over the world (MacDonald, 1986; Ho and Grooves, 1987; Goldfarb et al.,1988; Eisenlohr et al.,1989; Forster et al., 1996).

5.3 IRON ORE

A potential site for iron and its associated minerals of manganese is located at lat.12^{o} 03$^{'}$ 18.76$^{"}$ N and long. 06^{o} 51' 15.21"E in Bayan banki village. The site is located 7.5Km SE of Kwatarkoshi. BIF occurs interbedded with schist forming spines of the metasedimentary ridges in the area (Fig. 6). The BIF trends N-S, weathered and well exposed with an altitude of about 588 meters within the schist. The BIF is dark reddish brown, banded rock with alternation of light grey rich silica and darker iron-oxide rich bands.

Fe ore deposit is a principal raw material for the production of iron and steel. Iron ore is used for making cast iron, wrought iron and various steels for various purposes. It is also used for alloys with other metals for various uses.

Manganese in form of manganese oxides minerals (MnO) has a great economic significance as it is mostly used in the manufacturing of steel and ferro-manganese alloys. It is also used in the manufacturing of bleaching powder, insecticides and paints while some are used as cathodic material in dry-cell batteries. Manganese is mostly used in providing hardness to steel.

5.4 POTENTIAL SITE FOR OTHER MINERALS

Granite, granitic gneiss, gneiss, greenstone and granodiorites are the major rock types from the study area which do not present any major mineralization potential for economic minerals, but the associated minerals could be used for industrial purposes. For example, quartz from quartz veins characterizing the area could be used glass industry to manufacture glass and lenses. It can also be used for in the production of silicon chips in computers and wall clocks. Feldspars from aplite dykes and pegmatite are useful in ceramic industry. Soil clays which are weathered products of K-feldspars are also useful in ceramic, paint and pharmaceutical industries.

The granite, granitic gneiss, gneiss, greenstone and granodiorite from the study area could be quarried and crushed in to smaller gravels and fragments which could be used as building and construction materials. Sand and gravel which are the products of weathering of quartz and hard rocks occur as alluvium along stream and river channels in the study area. Sand may be an important source of glass and some placer deposits. Together with gravel, it could be used for concrete making and building construction (Fig. 6).

Laterite occurs in the central part of the study area at Bayan banki south of where the BIF is located in a seasonal stream channel, it may be used as aggregates for building and construction in place of clay bricks.

CHAPTER 6

SUMMARY, CONCLUSION AND RECOMMENDATION

6.1 SUMMARY

The Wonaka schist belt is located about 35 Km east of Maru schist belt and about 150 km west of Kazaure schist belt. The belt is within Lat. 11° 59' 50".25 N and Lat.12° 54' 25".00 and Long. 06° 40'.00"E and 07°10'.00"E. Most of the belt is within Sheets 54 (Gusau), 77 (Chafe) and 78 (Faskari).

The major lihologies found within the study area are; - granitic gneiss, gneiss, biotite- muscovite schist, BIF, hornfels, greenstone, granodiorite, medium grained biotite granite, porphyritic granite. diorite, phyllites and laterites as minor rock types.

Alumina (Al_2O_3) contents for all the rock types are generally within the range of (5.29-16.70 wt %). However, the rocks have aluminum saturation index [defined as the molar ratio of Al_2O_3/ ($CaO+Na_2O+K_2O$) after Ekwueme (2003)] greater than one (1) and consequently falls within the corundum norm except for the hornfels (sample 10) with Al_2O_3/ ($CaO+Na_2O+K_2O$) < 1 probably due to high content of CaO even greater than Al_2O_3, hence cannot have corundum in its norm.

N-S trending metasedimentary ridge in the area are composed of schists and phyllites interlayered with BIF. The BIF forms the ‘‘spine of the ridge’’ examples are located at lat.12° 03' 18.76" N and long. 06° 51' 15.21"E in Bayan Banki village. The BIF in the study area is of the silicate facie series. It is the most wide spread type of iron formation in Nigeria that is developed in all the schist

belt of northern Nigeria especially in the Malumfashi (Tudun kudu and Unguwar Malam Ayuba) , Birnin-Gwari schist belts, in Isanlu in Central Nigeria and that of Kazaure schist belt.

However, potential site for gold is located at lat.12^{o} 12$^{'}$54.00$^{''}$ N and long. 07^{o} 00' 26.21"E in river gajere at Butsa village.

6.2 CONCLUSION

Based on the geochemical data and discrimination diagrams presented earlier in this work, the granitic gneiss at Kwatarkwashi area is a paragneiss (sedimentary origin). Greenstone and the schist have also being shown to be sedimentary origin. On the other hand, the gneiss (ortho-gneiss) hornfels, granodiorites and the granites have igneous origin.

Trace element data have also shown that the BIF is enriched in Ni, Cr, Co and V this indicates that the BIF have dual provenance, terrigenous and submarine hydrothermal as basic-ultrabasic material was a major contributor to the basin of deposition.

Based on the variations in major, trace and lithophile element ratios in the BIF, it can be said that the material for the BIF is sourced from submarine hydrothermal with terrigenous contributions.

The present work has shown the presence of iron-ore in the form of BIF. Placer gold deposits is now present in Wonaka schist and documented in this work, though Woakes and Bafor (1983) presented the belt as barren of primary gold mineralization.

6.3 RECOMMENDATION

The dominance of oil on the Nigerian economy has not helped matters, therefore, a proper knowledge of the geology and accurate inventory of the mineral resource potential of Northern part of Wonaka schist belt and the documentation of this work/information in the form of thesis is

very necessary to update and contribute to knowledge of Wonaka schist belt and possibly attract public and private sector investors to the minerals sector of the Zamfara State economy and that of our beloved country, Nigeria, which in turn should lead to the establishment of small and medium-scale enterprises. Such enterprises will resuscitate economic activities that will lead to economic growth, employment generation, poverty reduction and social tranquility.

REFERENCES

Adekoya J.A. 1995. Supergene Fe-Mn enrichment in Precamrian Banded Iron Formation, Birnin-Gwari NW Nigeria *journal Min. geol*. Vol. 31 (1) pp. 63-72.

Adekoya J.A. 1996. The Nigerian schist belt: Age and depositional environment implications from associated banded iron-formations. *Journal Min. geol*. vol32 (1) pp 35-46

Ajayi, T.R. 1995. Moving average and trend surface analysis of regional geochemical data in Ife-Ilesha goldfield , S.W. Nigeria. *Journal of Min. geol*.Vol 31 (1). pp 21-38

Ajayi, T.R. 1998. Integrated exploration and statistical studies of geochemical data in Ife-Ilesha gold field. Unpublished Ph.D thesis, Obafemi Awolowo University. pp 461

Ajibade, A.C and Wright, J.B. 1989. The Togo-Benin-Nigeria Shield: Evidence of crustal aggregation in Pan-African belt. Tectenophysics, 165, pp. 125-129.

Akande, A.O and Kinnaird, J. 1990 Characterization and origin of ore-forming fluids in the Nigerian mineral belts. Proceedings of the Eighth Quardrennial IAGOD Symposium, Ottawa, Canada, pp199-218.

Akintola, O.F. and Adekeye, J.I. 2008. Mineralization controls and petrogenesis of rare metal pegmatites of Nasarawa area. Central Nigeria. *Earth Science Res. Journal*, Vol. 12 (1). Pp. 1-11

Ball, E. 1980. An example of very consistent brittle deformation over a wide continental area : The late Pan-African fracture systemof the Tuareg and Nigerian Shields. Techtenophysics, 61(4). Pp. 363-370.

Bonatti, E., Kraemer, T., Rydell, H. 1972. Classification and genesis of submarine iron manganese deposits In Horn, D.R. (E.d.), Conference of Ferromanganese Deposit on the Ocean Floor. Harriman New York, Anden House. Pp. 149-166.

Dada, S.S.1997. Proterozoic evolution of the Nigeria-Boborema province

Danbatta, U.A. 1999. The geotectonic evolution of the Kazaure schist belt in the Precambrian basement of NW Nigeria. Unpuclished Ph.d thesis, Ahmadu Bello University, Zaria, pp. 19-20, 24.

Danbatta, U.A. 2003. The tecteonic significance of the NNE- continuation of the Kalangai fault zone into Kazaure Schist Belt of NW Nigeria. *Science Africana*, Vol. 2(1 and 2), pp. 17-25.

Eisenlohr, D., Grooves, D.I., and Partington, G.A. 1989. Craton scale shear zones and their significance to Archean gold mineralization in *Western Australia. Mineral. Deposita* 24, pp. 1-8.

Ekwueme, B.N. 2003. The Precambrian geology and evolution of the southeastern Nigerian Basement Complex. pp. 30.

Forster, H., Koenemann, F.H. and Knittel, U. 1996. Regional framework for gold deposition of the Odzi-Maiturare-Manica greenstone belt, Zimbabwe, Mozambique. Trans. Instn.Min. Metall. (section B: Appl. Earth sci.); 105, B60-73.

Goldferb, R.J., Leach, D.L.,Pickthorn, W.J. and Paterson, C.J., 1988. Origin of lode-gold deposit of the Juneau gold belt southeastern Alaska. Geology, 16, pp.440-443.

Garba, I. 1988. The variety and possible origin of the Nigerian gold mineralization: Okolom-Dogondaji and Waya veinsas case studies.*Journal African. EarthSci*.,1981-1986

Garba, I. 1992. A rare earth elements(REE) study of Bin Yauri gold deposit, Nigeria. Trans. Inst. *Min. Metall.*80B:pp. 158-161

Garba, I. Akande, S.O.1992. The origin and significance of non-aqueous CO_2 fluid inclusions in the auriferous veins of Bin Yauri, northwestern Nigeria. Mineral Deposita 27: pp. 249-255.

Garba, I. 1996. Tourmalinization related to late Proterozoic-Early Palaezoic lode gold mineralization in the Bin Yauri area, Nigeria Minera. Deposita. 31, pp. 201-209.

Garba, I. 2000. Origin of Pan African gold mineralization at Bin Yauri, Nigeria. *Journal. African Earth Sci.*, 31, pp. 433-449.

Garba, I. 2005. Rare Earth Element (REE) and Lithophile element systematic used in tracing the origin of ore mineralisatiopn processes in the basement terrain of Nigeria. Afric. Geosci. Review, vol.12, 1-2, pp 69-78.

Harper, C.T., Sherrer, G., McCurry, P. and Wright, J.B., 1973. K-Ar retention ages from the Pan-African for Northern Nigeria. Bull. Geol. Soc. Am., 84:pp. 919-926.

Ho, S.E. and Groves, D.I. 1987. Recent advances in understanding Precambrian gold deposit. Geology Department and University Extension. University of Western Australia Publication, 11.

Ibrahim, A.A. 2002. Geological setting and the Geochemistry of iron-formation in the Kazaure schist belt NW Nigeria. Unpublished Msc thesis. A B U Zaria.

Khan R.M.K. and Naqvi S.M. 1996. Source processes for Archean Au-Ag vein deposits: evidence from lithophile elements systematic of Hollinger-McIntyre and Buffalo Ankerite deposits, Timmins *Canadian Journal Earth Sci*. Vol.26 pp.755-781.

Macdonald, A.J(ed.) 1986. Proceeding of gold 86. An International Symposium on the Geology of gold, Toronto, pp.517.

McCurry, P. 1973. The geology of degree sheet 21, Zaria, Nigeria. Overseas Geology and Mineral Reserves, No. 45.

McCurry, P. and Wright, J. 1971. On place and time in orogrnic granite plutonism. Geol. Soc. Amer. Bul. 82. Pp. 1713-1470.

McCurry, P. 1976. The geology of the Precambrian to lower Palaeozoic rocks of northern Nigeria-A review. In : Geology of Nigeria. (ed. C.A. Kogbe), Elizabethan Publ.Co. Lagos,pp. 15-40.

McCurry, P. and Wright, J. B. 1977. Geochemistry and calc-alkaline volcanic in northwestern Nigeria, and a possible Pan African suture zone. Earth planet. Sci. Lett, 37, pp. 90-96.

Mucke, A. 1994. Part 1. Post diagenetic ferruginization and sedimentary rocks (sandstone, oolitic iron stone , kaolins and bauxites) Including comparative study of the reddening of red beds.

Mucke, A. 2005. The Nigerian manganese-rich iron-formations and their host rocks — from sedimentation to metamorphism *African Journal. Earth Sci*. Vol 41, pp 407- 436.

Mucke, A., Annor A., and Neuman U. 1996. The Algoma type iron-formations of the Nigerian metavolcano-sedimentary schist belts. *Minerallium deposita* Vol.31, pp. 113-122.

Olayinka, I. 2009. Investment opportunities in solid minerals. Nigerian Tribune. Retrieved Thursday 19th February, 2009.

Okonkwo C.T. 1991. The petrology and Geochemistry of Koriga iron formation, NW Nigeria min.jn.b Vol.70 pp. 39-40.

Rahaman, MA; Ajayi, T.R,; Oshi, I.O and Asubiojo, F.O. 1988. Trace element geochemistry and geotectonic setting of Ife –Ilesha schist belt. In: Precambrian Geology of Nigeria. Published by Geological Survey of Nigeria, pp. 241-246

Rollinson, H. 1993. Using geochemical data: evaluation, presentation, interpretation. Longman Group, England, UK, pp. 133-303.

Russ W. 1957. The Geology of parts of Niger, Zaria and Sokoto Provinces Geol. Surv of Nigeria Bull. 27 pp. 37-41.

Tailor and Steven 1984. nwrc.usgs.gov/techrpt/sta13pdf.

Tailor, S.R. 1969. Trace element geochemistry of andesites and associated calc-alkaline rocks. Oregon Department. Geol. Min. Ind. Bull.,65. Pp. 43-60.

Tarney, J.1977. Petrology, Mineralogy and Geochemistry of the Falkland Plateau Basement Rocks, site 330, deep sea drilling project. Init. Rep36, pp.893-921.

Truswell JF, Cope RN (1963) The geology of parts of Niger and Zaria Provinces, Northern Geol Suvey of Nigeria Bull 29: pp.1–104.

Turner D.C., (1983) Upper Proterozoic schist belts in the Nigerian sector of the Pan-African Province of West Africa. Precambrian Res 21:pp.55–79.

Voelker et al.1979. U.S. Geological Survey and U.S. Bureau of Mines assessment reports. pp 97

Woakes M, Bafor B.E., (1984) Primary gold mineralization in Nigeria. In: *GOLD '82:* In: Foster RP (ed) The geology, geochemistry and genesis of gold deposits. Geological society of Zimbabwe, special publication No. 1. Balkema, Rotterdam, pp. 661-671.

Woakes M, Rahaman MA, Ajibade AC. 1987. Some metallogenetic features of the Nigerian basement. *Journal Afr Earth Sci* 6: pp.54–64.

Wright, J.B. 1976. Fracture systems in Nigeria and initiation of fracture zones in South Atlantic. Tectonophys., pp. 34, T43-47

APPENDICES

Appendix A

X-Ray Fluorescence Analytical Result

Comp/ELEM(ppm)	MA1	MA2	MA3	MA4	MA5	MA6	MA7	MA 8	MA9	MA10	MA11	MA12	MA13	MA14	MA15
Mg+/-	2.64	2.69	2.57	2.71	2.67	2.15	2.18	2.21	2.37	2.96	2.91	2.99	2.88	3.08	3.13
Al	63667	65531	65153.2	78778.6	75776.3	28002.2	23651.7	29653.2	26864.8	74359.9	71250.5	86121.9	87316.8	63389.2	63514.6
Si	394692.5	341872.3	370857.6	287116.9	297901.2	237265.1	226513.6	283127.3	285298.6	238531.6	347065.7	350817.4	34701.5	340595.9	313248
P+/-	5184	4123	6665	9735	8653	18477	18321	17892	18514	14893	8363	5541	5021	6949	7986
S+/-	716	722	893	1528	1419	3066	3021	2998	3056	1823	1121	767	701	950	1065
Cl+/-	239	259	300	524	597	945	943	973	976	514	390	253	215	303	389
K	36983	36012	50177	77715	76836	LOD	78932	72347	75261	683	52657	24623	23631	42137	48520
K+/-	358	345	483	878	653	471	462	432	460	103	547	280	272	433	539
Ca	6539	9110	10899	6882	6951	3440	3781	4550	4214	111994	20204	9978	9842	14593	7943
Ca+/-	105	80	149	161	172	165	171	183	173	1134	238	134	127	179	145
Ti	641	3815	915	7494	7541	5231	5483	5642	5393	5531	3075	1169	1076	2599	1966
Ti+/□	32	27	59	136	139	229	221	264	243	78	79	54	48	64	101
V	306.8	LOD	1069	646.9	380	152.2	136	LOD	LOD	300.1	525.8	645.1	543.1	436.6	354.6
Cr	12	17	38	149	96	156	148	110	148	79	95	43	LOD	24	95
Cr+/-	4	2	6	11	13	28	25	28	21	9	8	6	7	6	8
Mn	169	217	634	1054	1043	33871	35875	33956	34210	1084	492	391	342	337	1470
Mn+/-	6	5	11	19	18	573	523	521	542	19	11	8	8	8	20
Fe	5638	9665	10058	66582	67753	291109	29783	29843	29176	58798	27529	14858	14621	17324	44025
Fe+/-	45	53	80	637	621	4833	4321	4217	4634	559	228	114	111	137	381
Co	136	240	244	1369	761	LOD	LOD	LOD	LOD	1207	669	358	376	342	644
Co+/-	22	12	35	97	95	926	12	13	17	87	56	37	35	41	66
Ni	58	154	78	112	58	407	421	432	461	80	92	69	68	70	101
Ni+/-	15	13	17	25	19	49	46	47	43	24	20	17	16	17	20

Cu	LOD	58	86	172	165	349	321	376	351	134	139	84	76	86	41
$Cu^{+/-}$	29	11	11	15	14	25	24	29	21	14	13	11	12	11	11
Zn	83	77	168	195	187	210	220	235	243	94	109	80	81	95	156
$Zn^{+/-}$	6	4	8	10	12	14	18	16	13	8	8	7	6	7	8
As	LOD	LOD	LOD	LOD	LOD	LOD	LOD	LOD	LOD	LOD	11	LOD	LOD	LOD	LOD
Se	16.3	18.8	15.5	5.9	5.2	11	11	14	16	14.4	11.3	6.8	5.5	12	4.5
Rb	253	219	123	575	601	9.3	10	13	14	2.4	229	84	80	184	536
Sr	282	187	1506	243	211	29.5	22.4	30	27	212	1102	1414	1426	401	114
Zr	138	442	566	524	521	327	338	389	329	63	666	257	247	440	293
Mo	LOD	LOD	LOD	39	28	LOD	12	15	LOD	LOD	LOD	LOD	LOD	7	LOD
Ag	29	58	50	80	74	174	178	173	169	81	63	36	32	46	54
Cd	27	28	30	31	35	46	42	41	38	34	35	31	29	28	27
Sn	LOD	LOD	LOD	LOD	LOD	67	53	55	LOD	LOD	LOD	LOD	LOD	LOD	LOD
Sb	LOD	LOD	LOD	LOD	LOD	LOD	LOD	14	12	LOD	LOD	LOD	LOD	LOD	LOD
I	LOD	LOD	LOD	LOD	LOD	LOD	LOD	LOD	LOD	498	LOD	LOD	LOD	LOD	LOD
Ba	254	312	1487	983	822	1048	997	1072	1297	324	1056	953	514	701	566
Hf	44.6	49	LOD	LOD	56	LOD	LOD	LOD	LOD	57.9	LOD	40.7	LOD	LOD	LOD
W	346.5	310	320.4	135.4	160	312.3	289	LOD	337.6	180.1	188.8	191.5	201	246.5	128.5
Hg	103	87	92	52	35	80	111	LOD	55	55	52	36	68	64	29
Pb	46	71	68	49	27	LOD	LOD	LOD	LOD	LOD	55	52	LOD	39	42
Bi	41.3	78	42	51.2	38	36.4	29	28	33	LOD	52.5	16.5	LOD	77.5	49.1
LE	522982.1	512962.2	498591.4	469385	456873.9	421838.4	462136.6	381572.0	2203231.6	529969.5	500440.2	529145.1	523498.7	543049.9	543614.3

LOD= Limit of Detection

LE= Lower elements

APPENDIX B

Flame Photometry Analytical Result Alkali Elements for Rock Samples.

S/No	Sample ID	Na (ppm)	Uncertainty	K(ppm)	Uncertainty	Conversion Factor	Na(ppm)	K(ppm)
1	MA1	14.1	0.02115	15.3	0.0489	50	815	982
2	MA3	8.7	0.01305	7.3	0.0219	50	365	440
3	MA4	62.4	0.0936	117.9	0.3237	50	5395	6501
4	MA6	11.4	0.0171	3.2	0.0093	50	155	187
5	MA10	42	0.063	70.2	0.2106	50	3510	4230
6	MA12	32.5	0.04875	6.5	0.0195	50	325	392
7	MA13	10.8	0.0162	8.9	0.0267	50	445	536
8	MA14	14.9	0.02235	19	0.057	50	950	1145
9	MA15	29.4	0.0441	39.3	0.1176	50	1960	2362

APPENDIX C

Location and joint directions of some of the sample areas.

Locations	Joint Directions
MA1	194^o, 209^o, 330^o, 210^o, 110^o, 109^o, 198^o, 255^o,102^o,077^o,029^o, 015^o, 266^o,270^o,344^o,230^o, 255^o,320^o , 355^o,270^o,320^o, 201^o,212^o .
MA3	052^o, 010^o, 007^o, 012^o, 028^o, 101^o, 290^o.
MA10	215^o, 216^o, 230^o, 290^o, 310^o, 125^o.
MA14	189^o, 063^o.074^o,210^o,260^o,119^o,187^o,288^o,310^o,265^o,270^o,189^o,193^o,168^o,330^o.
MA15	063^o, 074^o, 210^o, 260^o, 119^o,187^o,320^o.

$0\text{-}180^o$	Frequency (F1)	$181\text{-}360^o$	Frequency (F2)	FI+F2= F	F%
0-30	6	181-210	11	17	26.15
31-60	1	211-240	7	8	12.31
61-90	4	241-270	8	12	18.46
91-120	9	271-300	4	13	20.00
121-150	2	301-330	8	10	15.39
151-180	3	331-360	2	5	7.70